Supporting Information

Microenvironment Modulation of Zr Sites in Covalent Organic Frameworks for Low-Pressure Preparation of UHMWPE

Hao-Tian Li, ‡[a] Tao Zhou, ‡[a] Yu-Qing Peng, ‡[b] Xiao-Ke Shi, ‡[c] Zhi-Hao Zhu, [a] Ye-Bin Guan, [a] Yong-Qing Li, *[b] Zhen Liu*[c] and Chuan-Lei Zhang*[a]

(‡ These authors contributed equally to this work.)

[1]Anhui Provincial Key Laboratory of Advanced Catalysis and Energy Materials, Anhui Ultra High Molecular Weight Polyethylene Fiber Engineering Research Center, School of Chemistry and Chemical Engineering, Anqing Normal University, Anqing 261433, P. R. China. E-mail: clzhang@nju.edu.cn.

[2]State Key Laboratory of Polyolefins and Catalysis, Shanghai Key Laboratory of Catalysis Technology for Polyolefins, Shanghai Research Institute of Chemical Industry Co., Ltd, Shanghai 200062, P.R. China. E-mail: liyongqing@srici.cn.

[3]School of Chemical Engineering, East China University of Science and Technology, Shanghai 200237, P.R. China; Email: liuzhen@ecust.edu.cn.

Corresponding authors: clzhang@nju.edu.cn.

CONTENTS

1. General Information

1.1 Materials

All materials, commercially available solvents and reagents purchased from Energy Chemical, Bide Pharmatech, etc., were used without further purification unless otherwise indicated.

Agilent columns dewatered and deoxygenated ethylene (ETH, > 99.99%), and 4A molecular sieves dewatered and treated toluene (MB, < 30 ppm). 4-aminobenzyl cyanide and 4-aminobenzonitrile were purchased from Bide Pharmatech Ltd. trifluoromethanesulfonic acid was purchased from Energy Chemical.

1.2 Measurements

Powder X-ray diffraction (PXRD) was collected on a Rigaku Miniflex 600 rotating anode X-ray diffractometer equipped with graphite monochromatized Cu Kα radiation (λ = 1.54 Å). The morphology of the samples was characterized by a field emission scanning electron microanalyzer (SU-8600, Hitachi, Japan). Image elemental analysis (EA) was performed on an energy dispersive X-ray spectrometer (ELECT SUPER (C5), EDAX Inc.). The adsorption isotherm of nitrogen was determined at 77 k using a fully automated volumetric adsorption unit (Micromeritics ASAP 2060). The Zr content was quantified using an inductively coupled plasma atomic emission spectrometer (ICP-AES) with a PerkinElmer Optima 8000 model. IR spectra were recorded on an AVATAR 360 infrared spectrometer and the samples were pressed into pieces using KBr as a carrier. X-ray photoelectron spectroscopy (XPS) measurements were carried out on an ESCALAB 250 high-performance electron spectrometer using an excitation source of monochromatized Al Kα (hν = 1486.7 eV).X-ray absorption spectroscopy measurements were carried out at the National Synchrotron Radiation Research Center (NSRRC) on a Spring-8 (Japan) 12B2 Taiwan beamline. All data were collected in transmission mode for the metal foils and by fluorescence mode for the other samples. Data reduction, analysis and fitting were

performed using Athena and Artemis software packages. Energy calibration of the catalysts was performed by means of standard metal foils.

^{1}H NMR and ^{13}C NMR spectra were recorded at ambient temperature on a JEOL JNM-ECZR (^{1}H:500 MHz, ^{13}C:125 MHz) spectrometer.1H NMR analysis of polymers was carried out using a 5wt% polymer solution in an NMR tube of 1,2,4-trichlorobenzene at 125°C using a 30° pulse of 50.0 μs, a 10kHz spectral width, 5.0 s relaxation time and 3.2 s acquisition time. Quantitative ^{13}C NMR analysis of the polymer was performed at 125°C using a 10wt% polymer solution in an NMR tube of 1,2,4-trichlorobenzene using a 30° pulse of 16.8 μs, a spectral width of 20 kHz, a relaxation time of 2.0 s, an acquisition time of 0.65 s, and reverse gated decoupling. The samples were preheated for at least 30 min prior to data acquisition.

Molecular weights and molecular weight distributions of the polymers were determined by gel permeation chromatography (GPC) on a PL-GPC-220 equipped with two Agilent PLgel-Olexis columns using 1,2,4-trichlorobenzene as solvent at 150 °C. The calibration curves were constructed from polystyrene standards. The calibration curve was constructed from a polystyrene standard and generalized to linear polyethylene using Rudin's Mark-Houwink parameters: polyethylene's K=5.90×10^{-2} cm^3/g and α = 0.69. 1,2,4-trichlorobenzene (TCB) was selected as the eluent at a flow rate of 1.0 mL/min and a temperature of 150°C. Samples were prepared in TCB at a concentration of approximately 1-2 mg/mL and heated at 150°C for 24 h prior to injection.

The melting points of the polymers were measured on a TA Instruments DSC Q100 over a temperature range of 30-160°C at a heating and cooling rate of 10°C/min. Scans were performed according to the following steps: (1) Heat from 30.00°C to 160.00°C at 10.00°C/min; (2) Cool from 160.00°C to 30.00°C at 10.00°C/min; (3) Heat from 30.00°C to 160.00°C at 10.00°C/min.

Structural models of TbDa, TtDa, and metallization were generated using the Zeo++ program. The initial cell size was set to the theoretical parameters. Atomic

positions and total energies were repeatedly optimized using the Forcite module of Materials Studio. Finally, the lattice parameters were optimized iteratively using the Le Bail refinement method until the R_{WP} values were less than 5% and the refined profile showed good agreement with the experimental results.

2. COFs Synthesis and Characterization

2.1 Synthetic COFs monomers

1,3,5-Tris (4-nitrophenyl) benzene (*Tb-NO₂*). 4-nitroacetophenone (25 g), toluene (100 mL), and CF_3SO_3H (2 mL) were added to a flask equipped with a cooling condenser. Under N_2 atmosphere, the mixture was refluxed for 48 h. After cooling down to room temperature, the mixture was filtered to yield a black solid product. It was washed with DMF under refluxing and filtered. This procedure was carried out twice more, and a pale-yellow solid was obtained after drying. This product is insoluble in any common solvent. Yield: 19.83 g (89%).

1,3,5-tris-(4-aminophenyl)benzene*(Tb)*. A suspension of 1,3,5-tris(4-nitrophenyl)benzene (10.0 g, 22.7 mmol) and Pd/C (10wt%, 2.0 g) in ethanol (200 mL) was heated to reflux. After 1 h, hydrazine hydrate (30 mL) was added dropwise, and the mixture was refluxed overnight. The hot solution was filtered through diatomite ($\approx$ 2 cm thick) and left undisturbed to fully crystallize the product. The solid was filtered and washed with cold ethanol. Yield: 6.94 g (87%). MS (ESI+) m/z = 393 (M + CH_3CN + H), ¹H NMR (400 MHz, d_6-DMSO, 298K, TMS): δ 7.48 (d, 9H, J = 8.4 Hz), 6.66 (d, 6H, J=8.4 Hz), 5.24 (s, 6H) ppm.
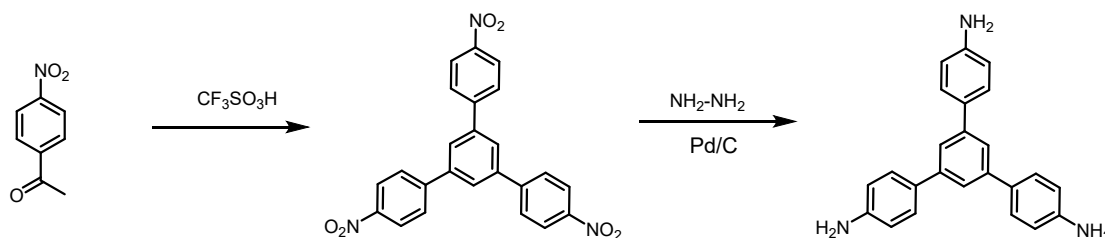
Figure S1. The synthesis route of **Tb.**

2,4,6-tris(4-aminophenyl)-1,3,5-triazine (*Tt*). Tt was synthesized via superacid

catalyzed trimerization of 4-aminobenzonitrile. In a typical synthesis, 100 ml of dichloromethane was added to a round-bottomed flask at 0ºC, 9 mL (100.00 mmol) trifluoromethanesulfonic acid was added slowly, the two solvents stirred in an inert atmosphere for 2 hours. Then 3.54 g (30.0 mmol) 4-aminobenzonitrile dissolved in 80 ml of chloroform was dropped into the above solvents in the form of bubbling, about 30 minutes. The resultant mixture was stirred for 48 h at room temperature in inert atmosphere. After that, 100 mL distilled water was added to the mixture and it was neutralized by adding 2M NaOH solution until the pH reaches to 7. Initially, with increase in pH, the orange precipitate dissolves to give a bright orange solution, which upon further increase in pH gives a pale-yellow precipitate. The resultant pale-yellow product was filtered and washed several times with distilled water. Yield: 3.19 g (90 %). MS (ESI+) m/z = 355 (M+H), ^{1}H NMR (400 MHz, d$_6$-DMSO, 298K, TMS): δ 8.34 (d, 6H, J = 8.8 Hz), 6.68 (d, 6H, J=8.8 Hz), 5.91 (s, 6H) ppm.
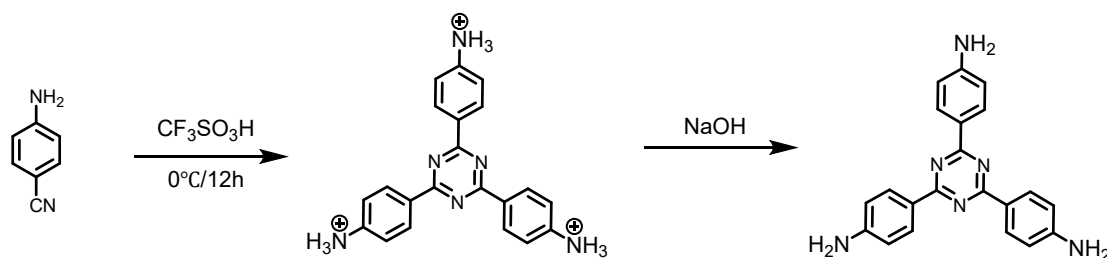
Figure S2. The synthesis route of **Tt.**

2,5-Dihydroxyterephthalaldehyde (Da). Purchased from Shanghai Aladdin Biochemical Technology Co. No further purification was performed. MS (ESI−) m/z = 165 (M + H), ^{1}H NMR (400 MHz, d$_6$-DMSO, 298K, TMS): δ 10.30 (d, 4H, J = 7.6 Hz), 7.22 (s, 2H) ppm.

2.2 COF and Zr-COF synthesis routes
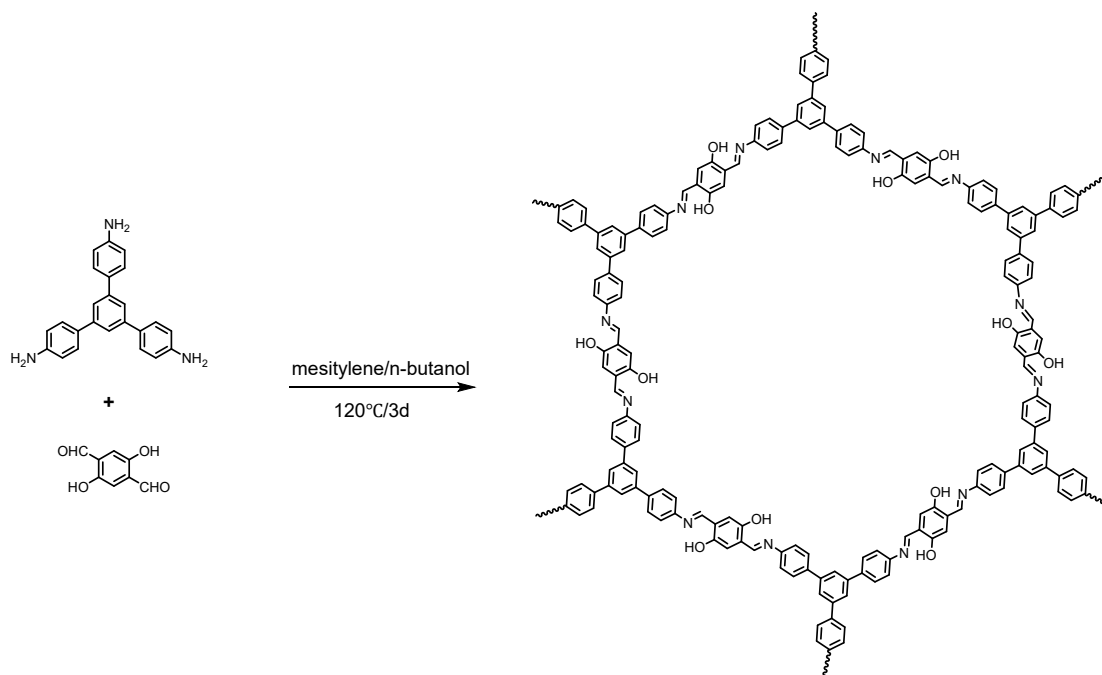
Figure S3. The synthesis route of **TbDa.**
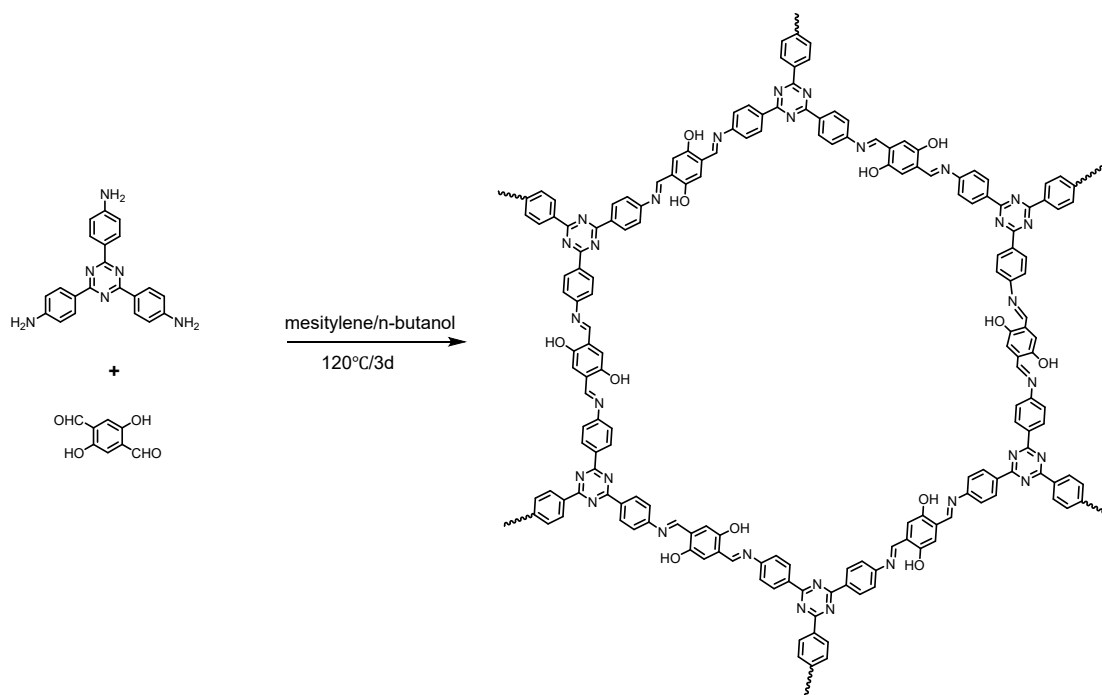
Figure S4. The synthesis route of **TtDa.**
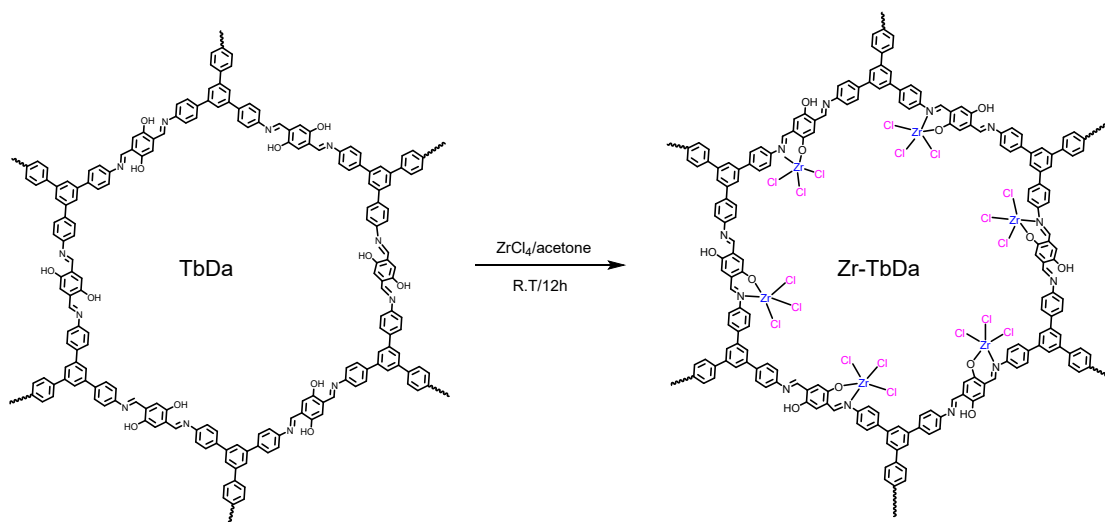
Figure S5. The synthesis route of **Zr-TbDa.**
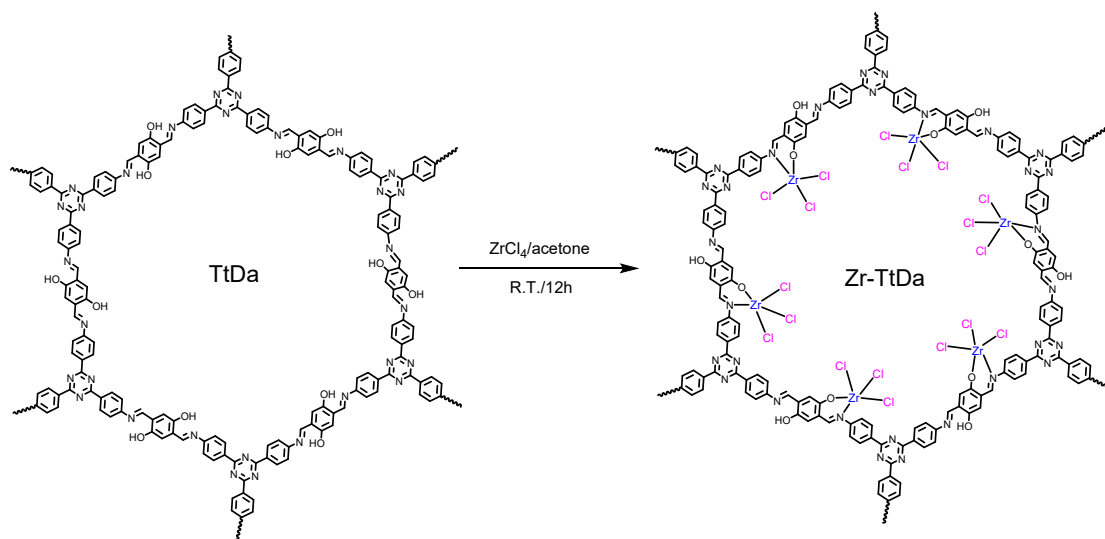
Figure S6. The synthesis route of **Zr-TtDa.**

2.3 Related Characterization Charts
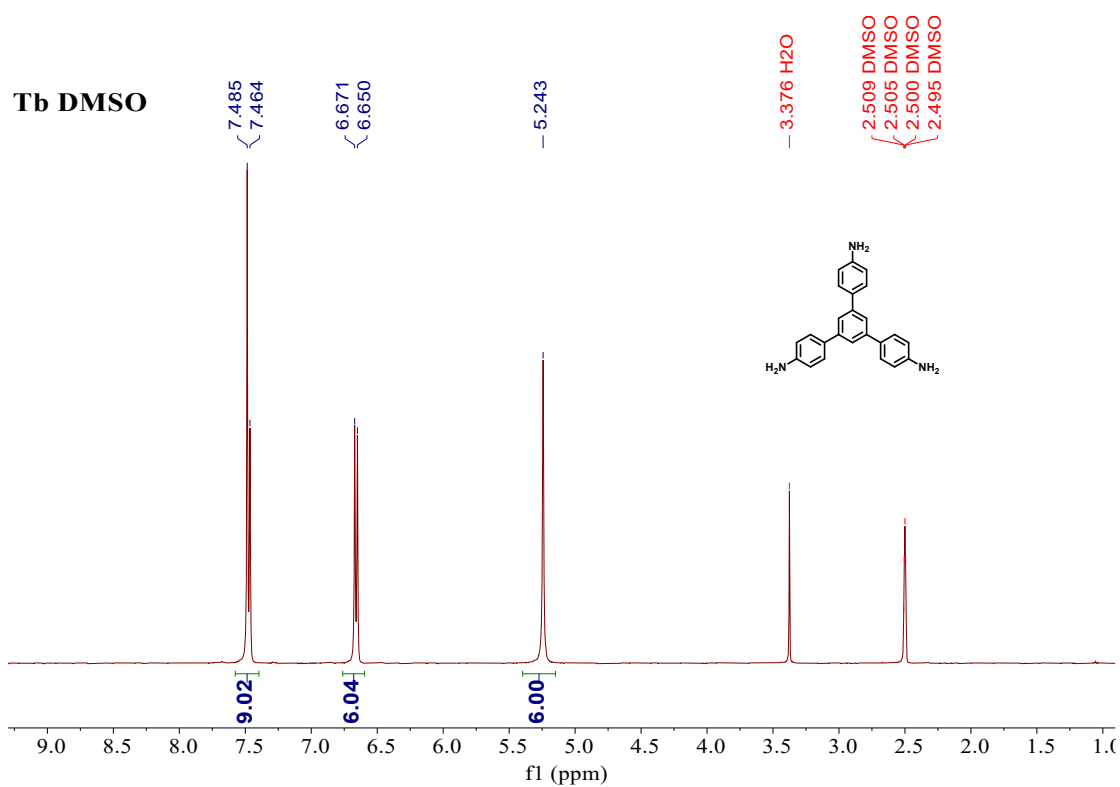
Figure S7. ^{1}H NMR spectrum of **Tb** (400 MHz, d[6]-DMSO, 298K, TMS).
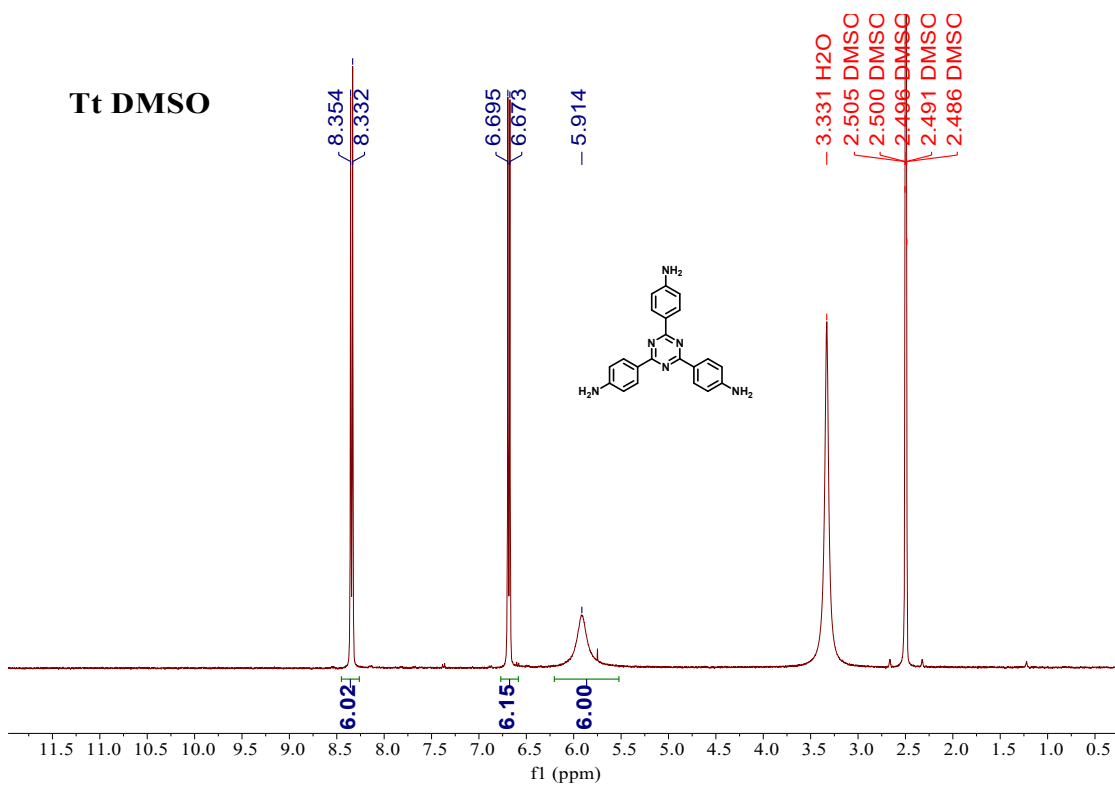
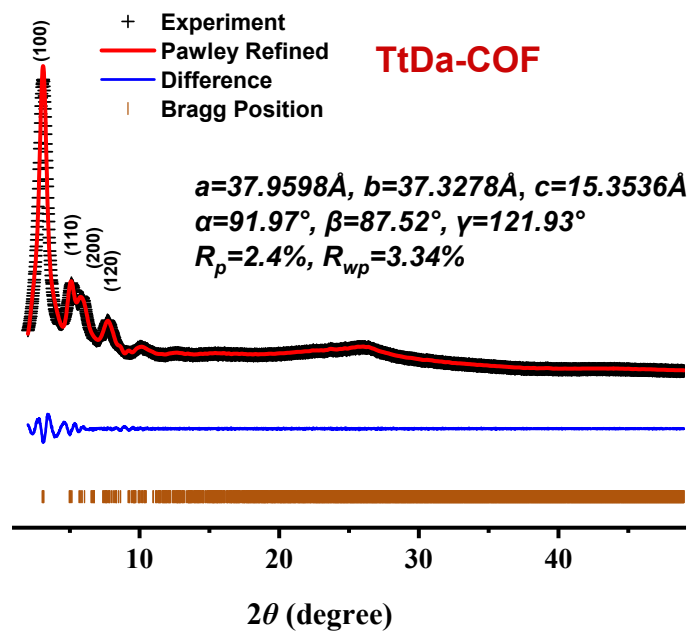**Figure S8.** ^{1}H NMR spectrum of **Tt** (400 MHz, d$_6$-DMSO, 298K, TMS).
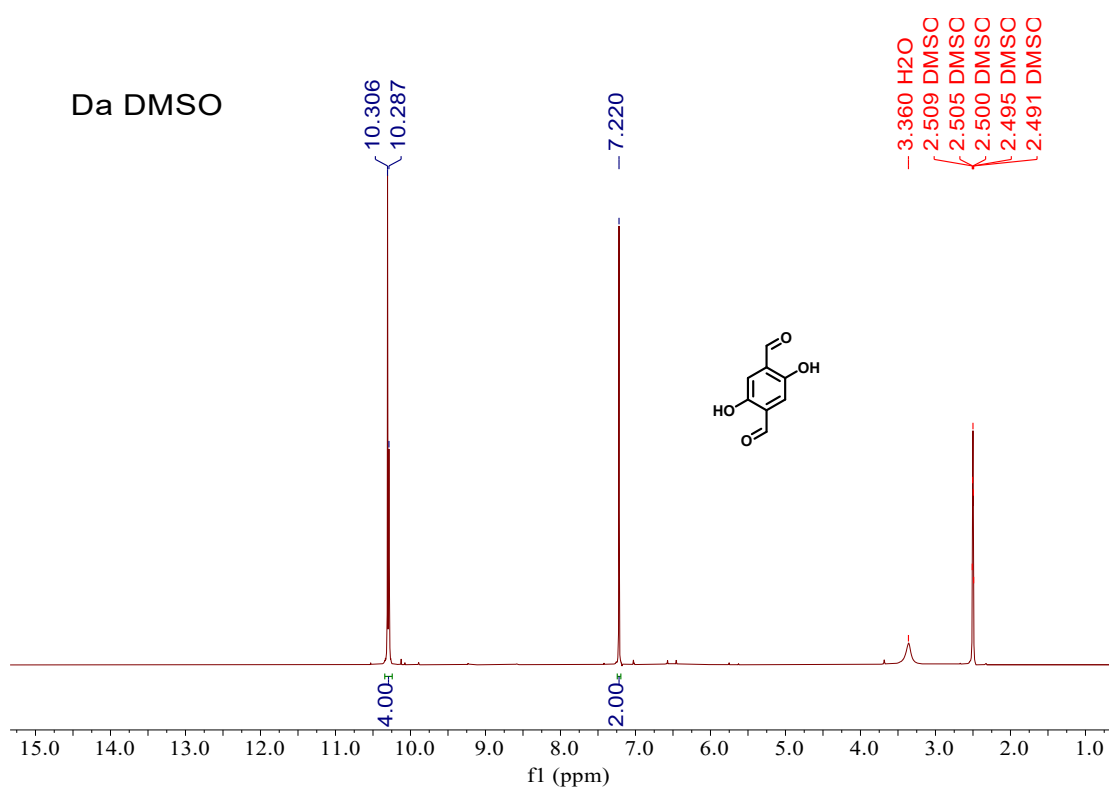
Figure S9. ^{1}H NMR spectrum of **Da** (400 MHz, d$_6$-DMSO, 298K, TMS).

Figure S10. PXRD patterns of **TtDa**.
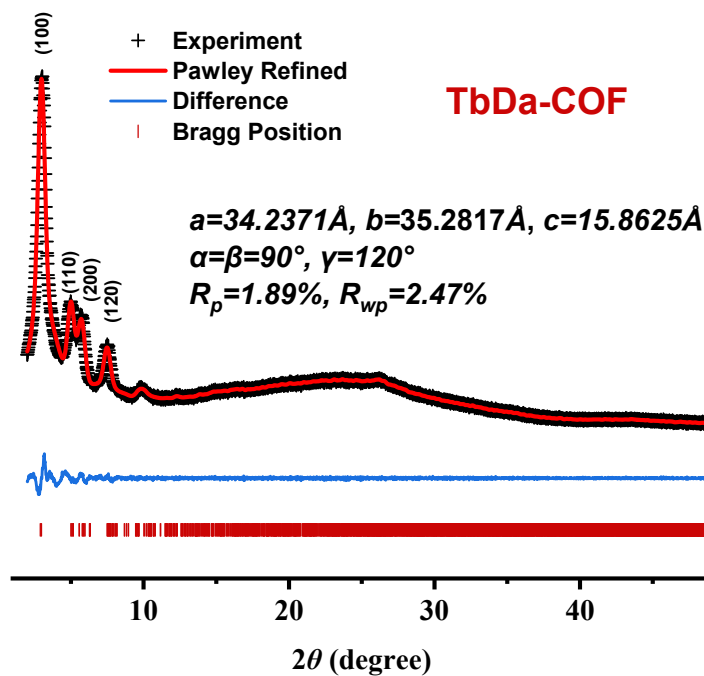
Figure S11. PXRD patterns of **TbDa**.
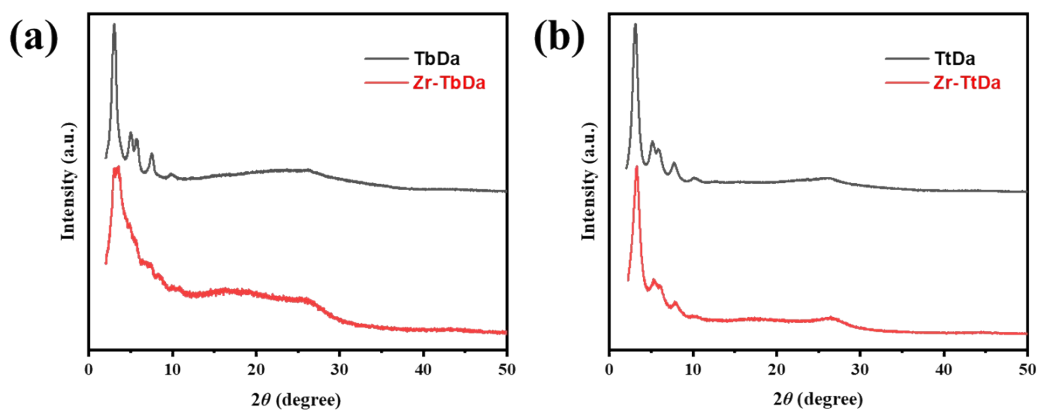
Figure S12. PXRD pattern of (a)**Zr-TbDa**, (b) **Zr-TtDa**.
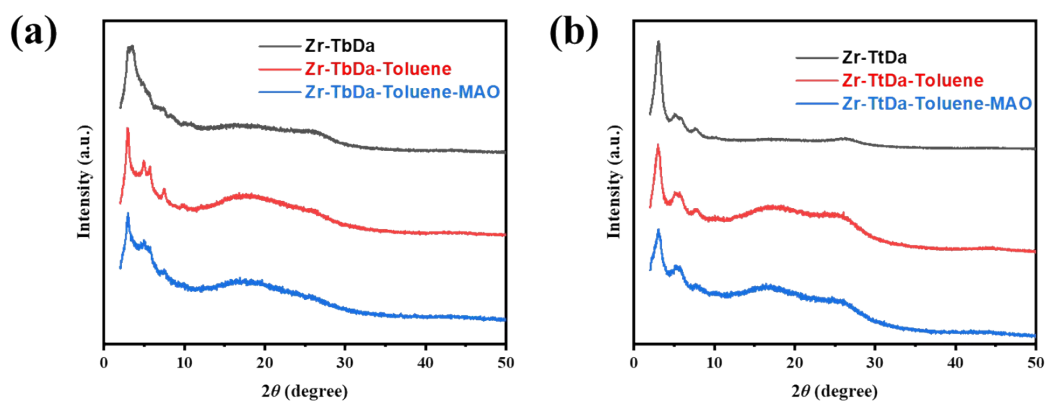
Figure S13. Stability test of **Zr-COF** in toluene solvent and toluene solvent containing MAO (Conditions: 100°C, 4h, 0.5MPa N_2).
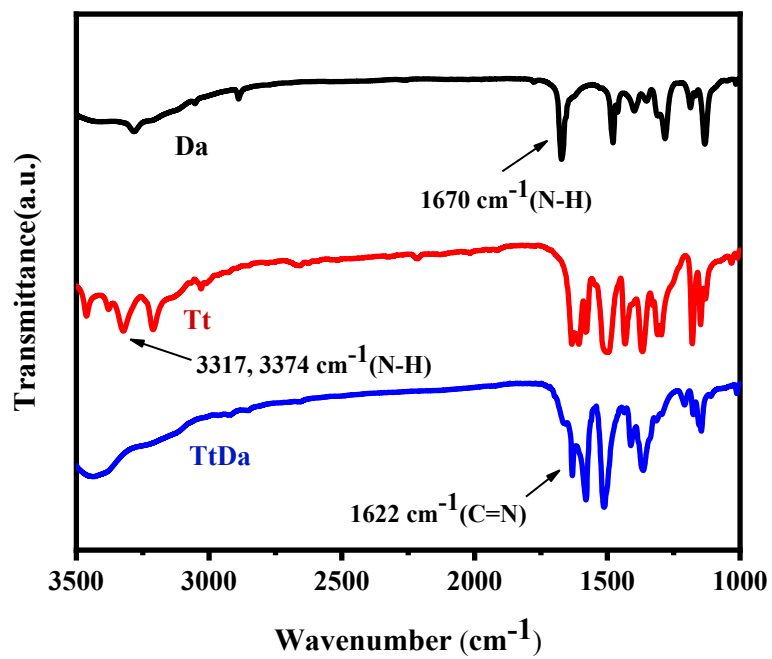
Figure S14. IR spectra of **TtDa-COF**.
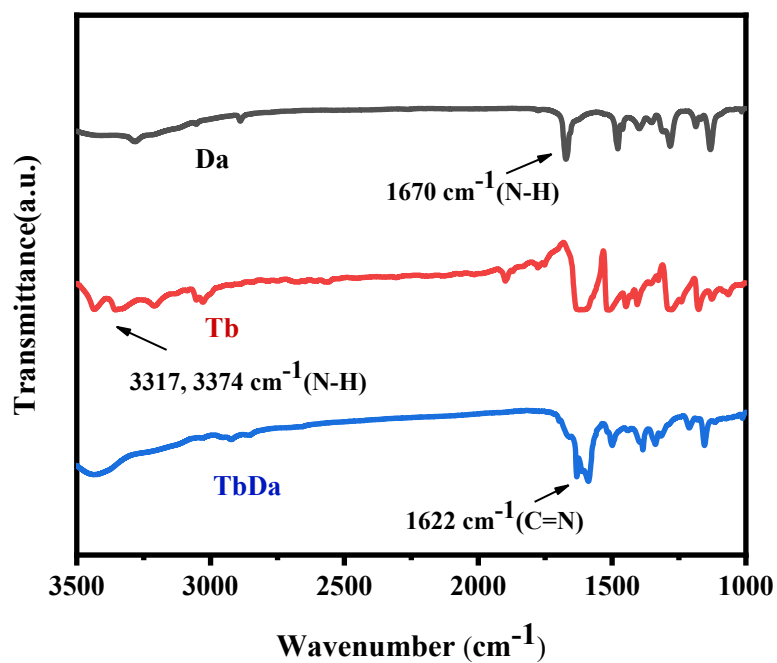
Figure S15. IR spectra of **TbDa-COF**.
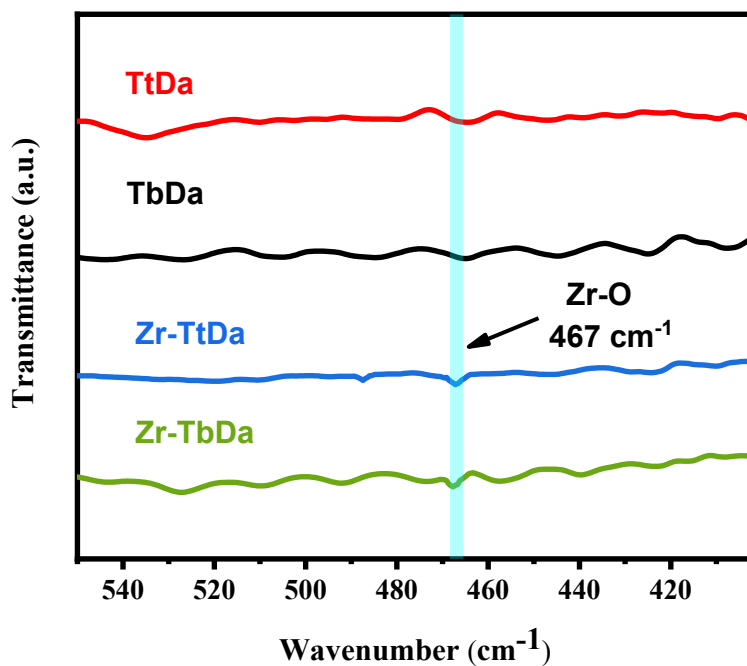
Figure S16. COF and **Zr-COF** infrared fingerprint area spectrums.

.
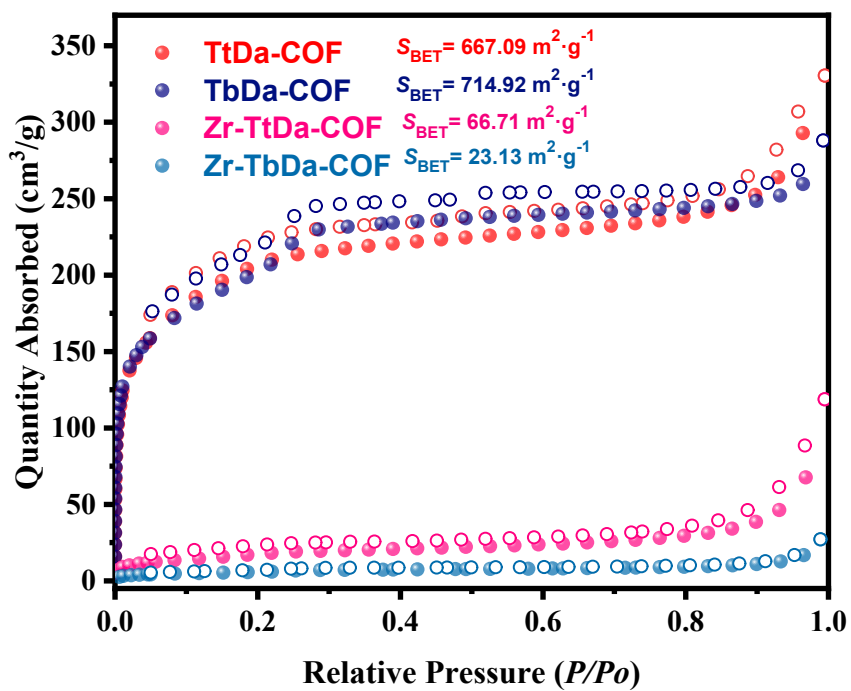
Fig

ure S17. N_2 adsorption-desorption isotherms at 77 K for **COF** and **Zr-COF**.
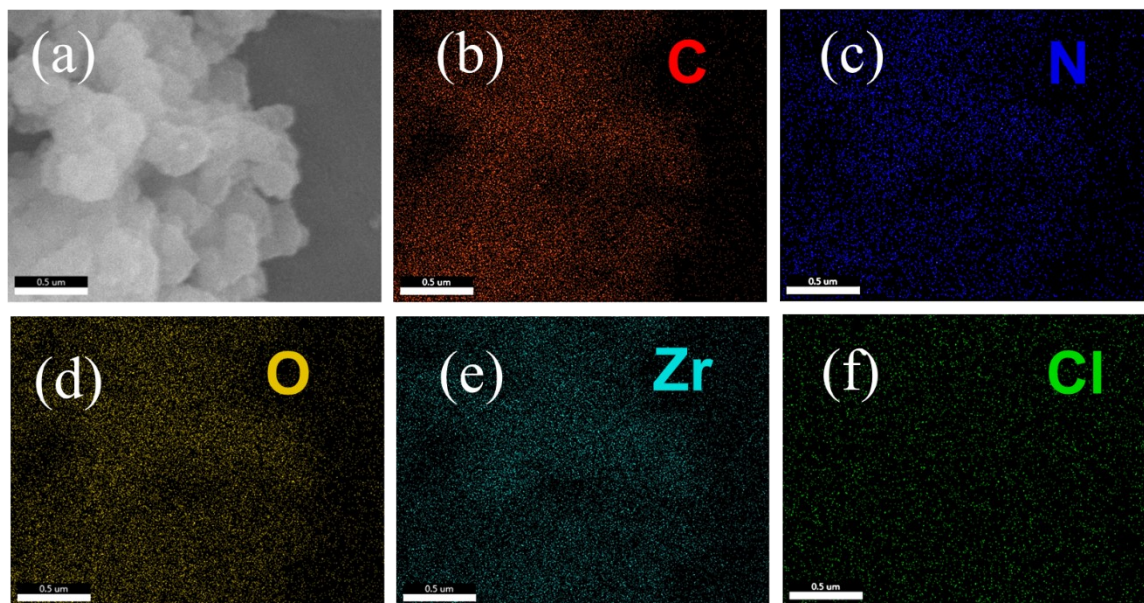
Figure S18. Elemental mapping of **Zr-TbDa.**
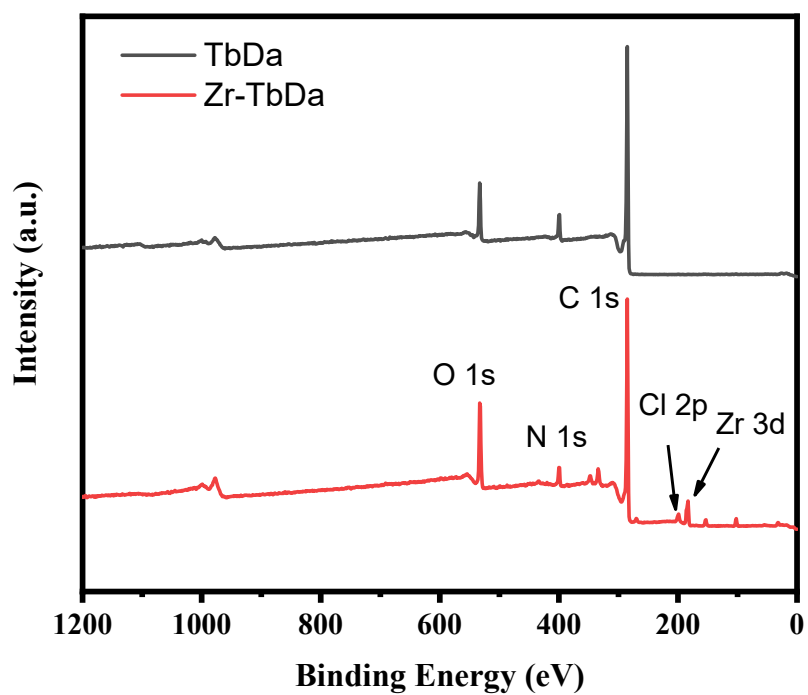
Figure S19. Survey spectrum of **TbDa** and **Zr-TbDa**.
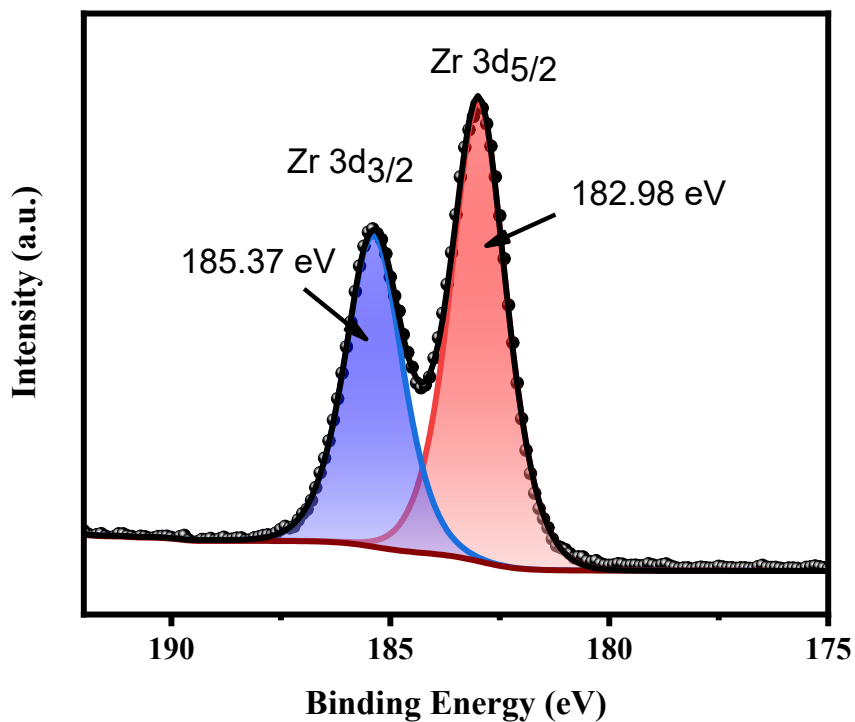
Figure S20. High-resolution Zr 3d XPS spectra of **Zr-TbDa**.
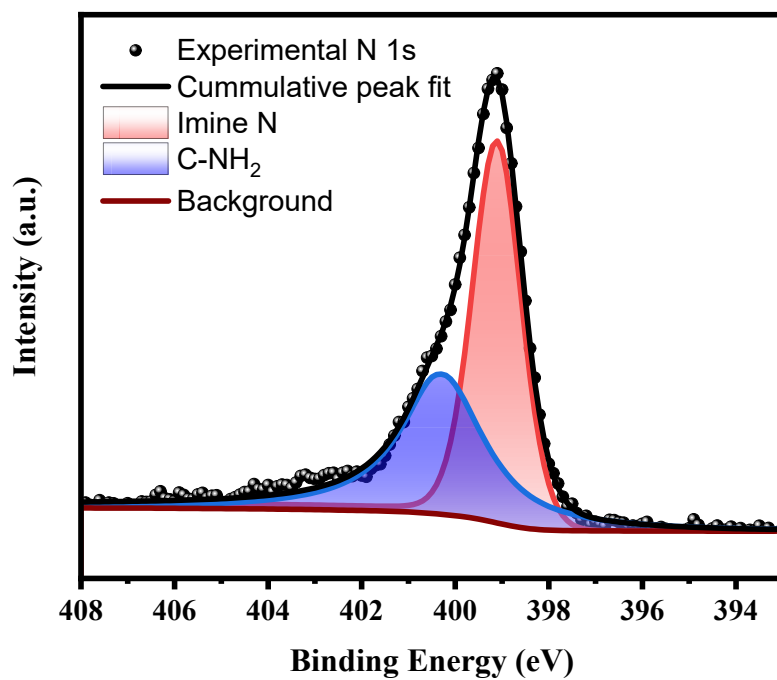
Figure S21. High-resolution N 1s XPS spectra of **TbDa**.
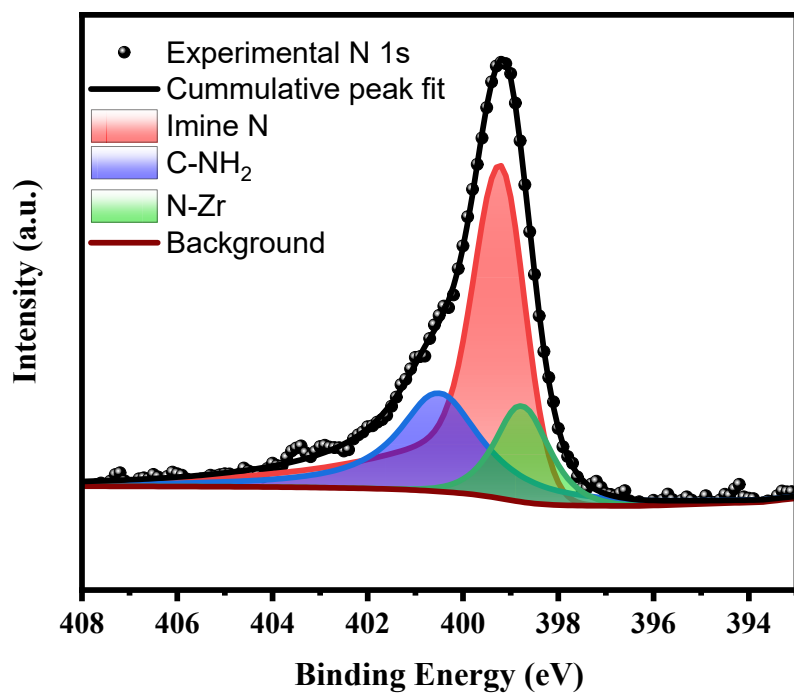
Figure S22. High-resolution N 1s XPS spectra of **Zr-TbDa**.
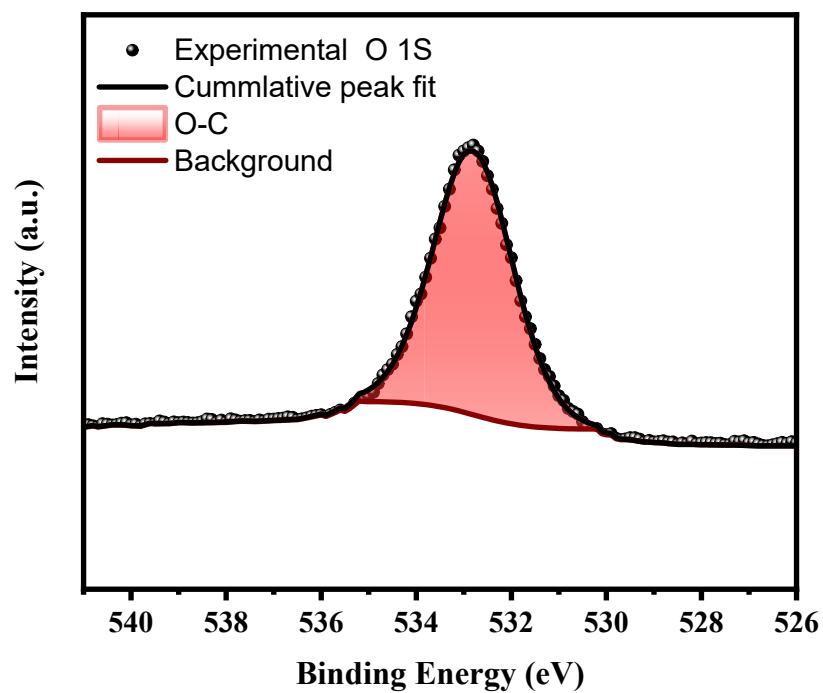
Figure S23. High-resolution O 1s XPS spectra of **TbDa**.
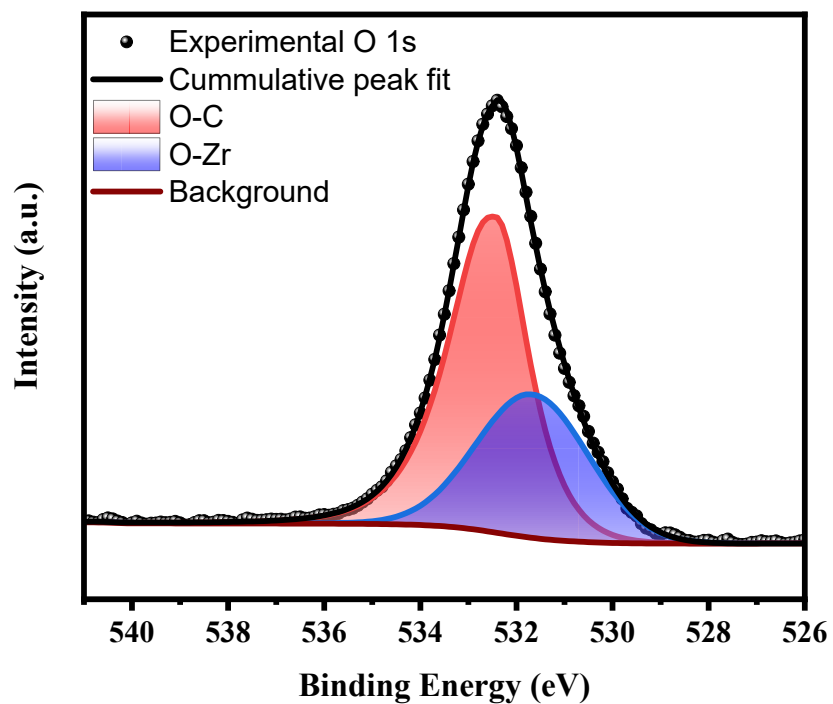
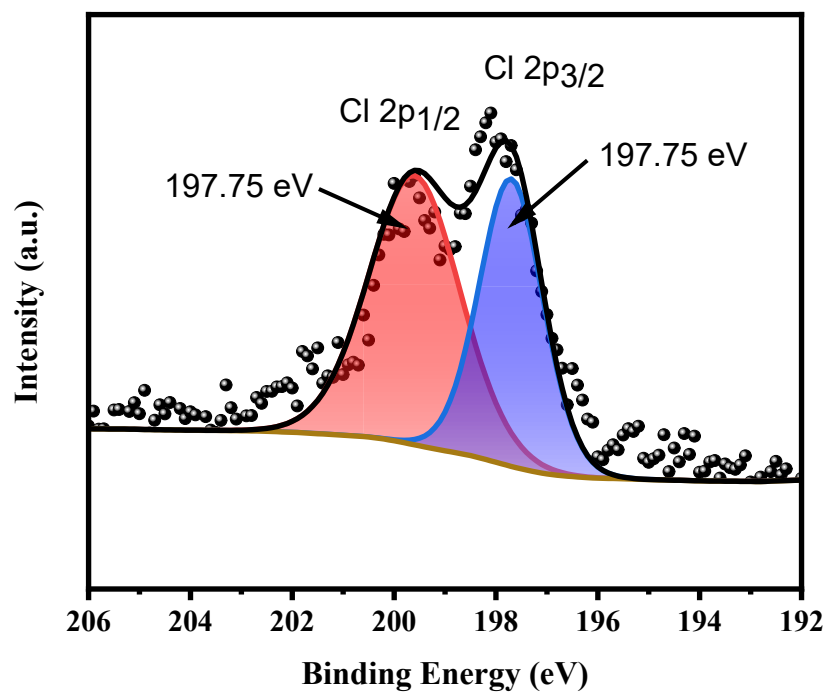**Figure S24**. High-resolution O 1s XPS spectra of **Zr-TbDa**.

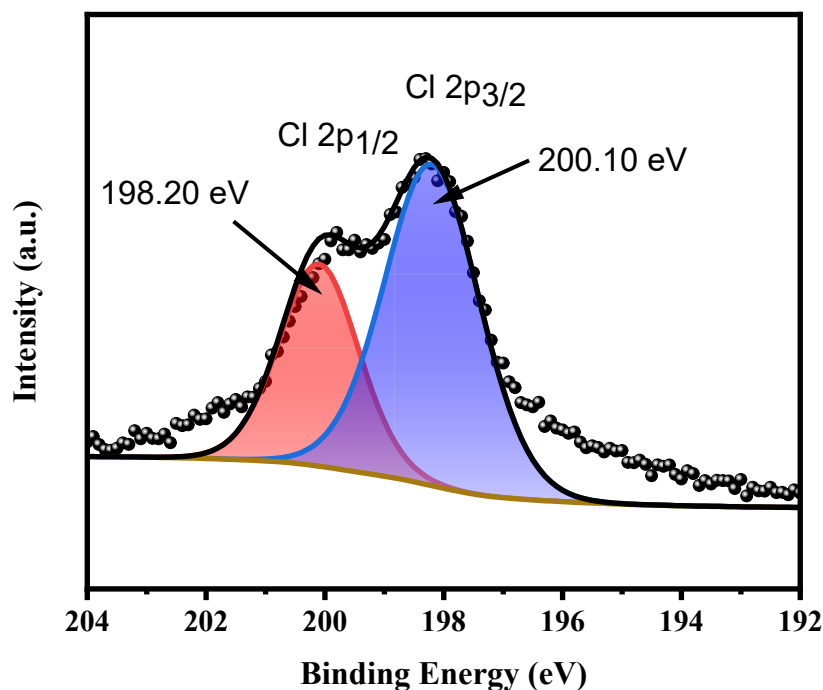**Figure S25**. High-resolution Cl 2p XPS spectra of **Zr-TtDa**.

Figure S26. High-resolution Cl 2p XPS spectra of **Zr-TbDa**.

3. General Procedure for Olefin Polymerization

Drying of Toluene Solvents

The purchased 4A molecular sieves were placed in a vacuum drying oven and dried under vacuum at 200°C for 8 hours. Immediately after completing the drying, it was stored in a sealed solvent canister with the molecular sieves about 1/3 of the volume of the solvent canister and toluene solvent was added. In addition, the molecular sieves were protected by passing N_2 during cooling and storage to prevent absorption of moisture from the air. The water content of the toluene solvent is checked, and subsequent polymerization operations can be performed only if the water content is less than 30 ppm.

Polymerization of Ethylene

The polymerization reaction was carried out in a stainless-steel high-pressure reactor (250 mL capacity) equipped with a mechanical stirrer and a pressure and temperature

control system under specified ethylene pressure conditions. First, the autoclave was baked under vacuum at 100°C for 12 hours, followed by three gas replacements with nitrogen. When the desired temperature was reached, 30 mL of dry toluene solvent was injected into the reactor, followed by addition of the desired amount of co-catalyst (MAO), and finally Zr-COF catalyst dissolved in the toluene solvent. After 5 min of reaction, the autoclave was pressurized to the desired ethylene pressure and vigorously stirred at 500 revolutions per minute. After the required reaction time, the ethylene pressure was released and the reaction mixture was quenched using 10% hydrochloric acid-ethanol. The polymer was collected, washed with ethanol and then dried under vacuum at 100°C and weighed.

Ethylene Polymerization Activity Calculation

Activity ($g_{PE} \cdot mol_{Zr}^{-1} \cdot h^{-1}$) = mass of polymer isolated/(mol $_{Zr}$ in Zr-COF catalyst $\times$ experiment duration)

Table S1. Catalytic polymerization of ethylene by **Zr-TtDa** at different Al/Zr ratios and characterization of the resulting polymers.

entry	catalyst	[Al]: [Zr]	pressure	temperature	activity ($\times 10^4$)
1	**Zr-TtDa**	300:1	10 bar	100°C	/[a]
2	**Zr-TtDa**	500:1	10 bar	100°C	2.21
3	**Zr-TtDa**	1000:1	10 bar	100°C	6.52
4	**Zr-TtDa**	1500:1	10 bar	100°C	7.92
5	**Zr-TtDa**	2000:1	10 bar	100°C	7.06

[a] Polythene product not collected.

4. Characterization of Polymerization Products

Zr-TbDa-5bar

Figure S27. ^{1}H NMR spectrum of polyethylene produced from Zr-TbDa (500 MHz, 1,2,4-Trichlorobenzene, 125°C). Table 1, entry 1.
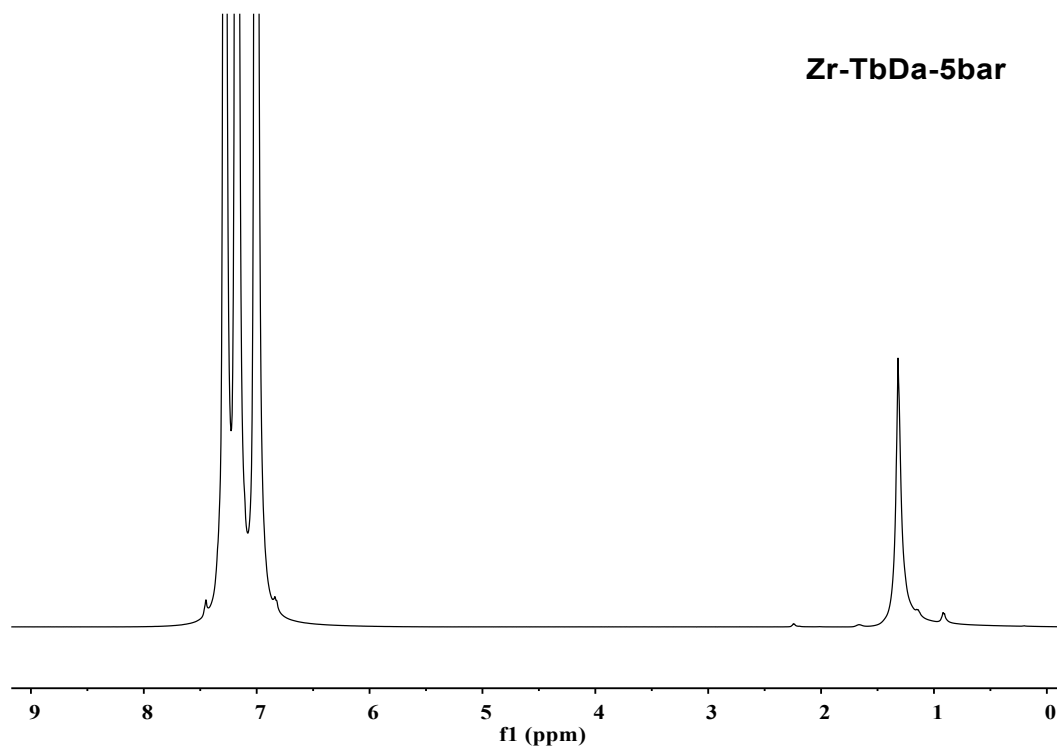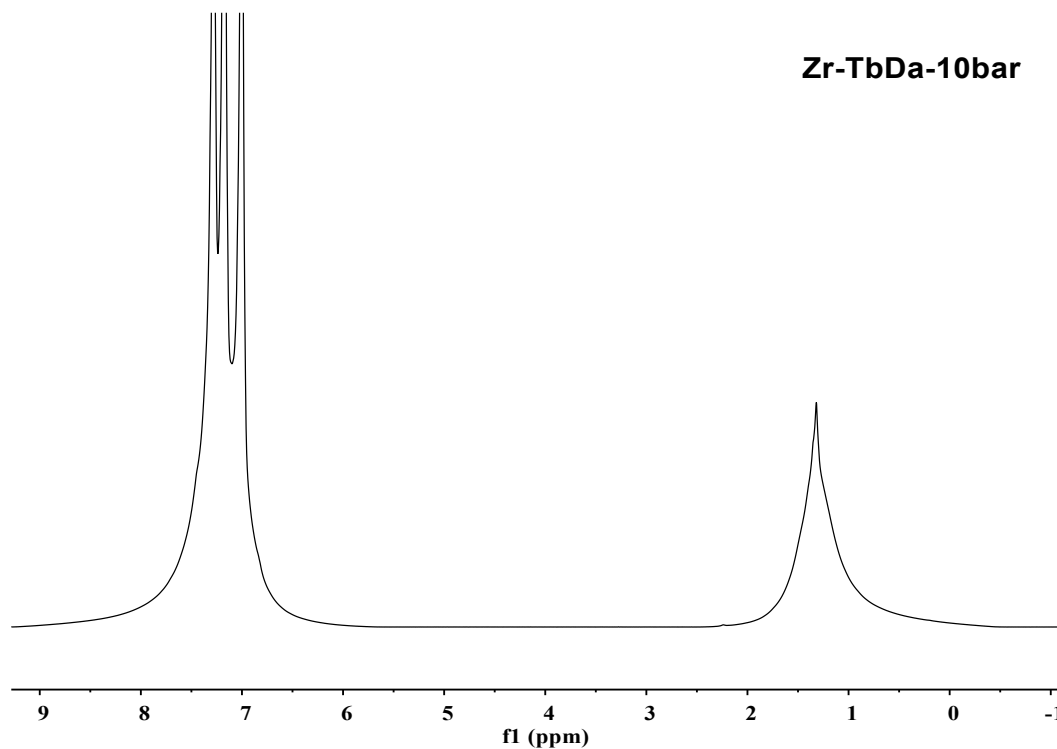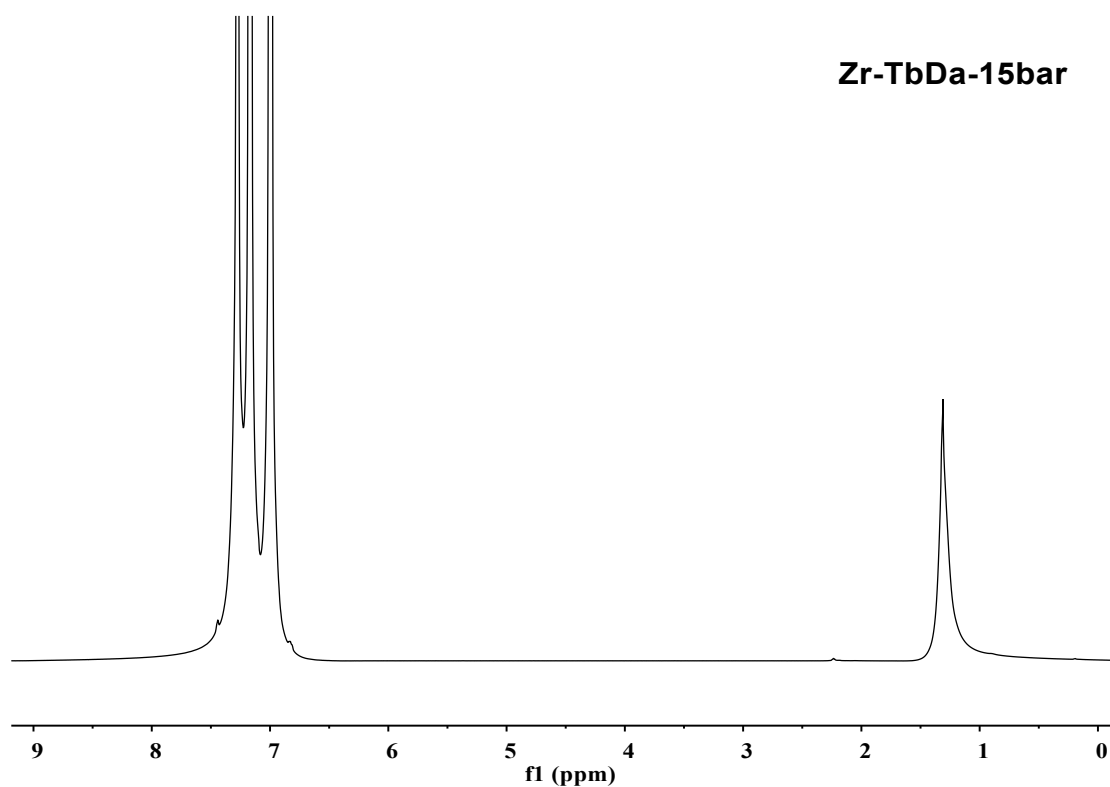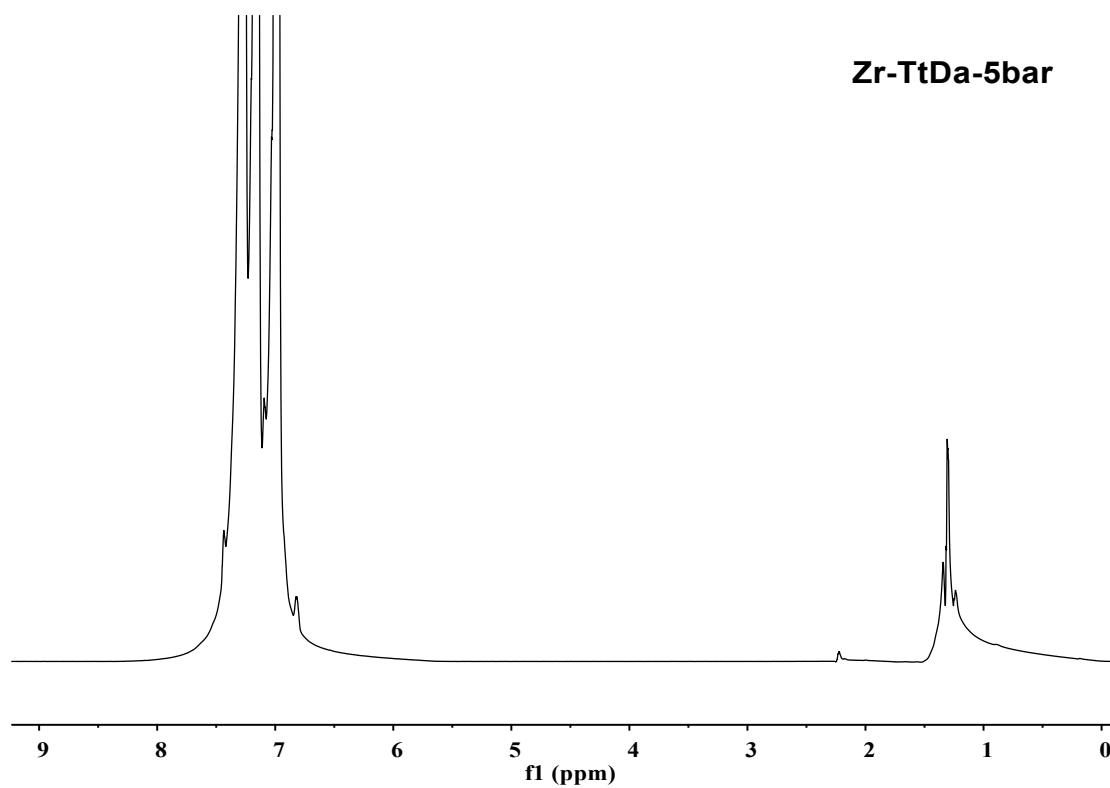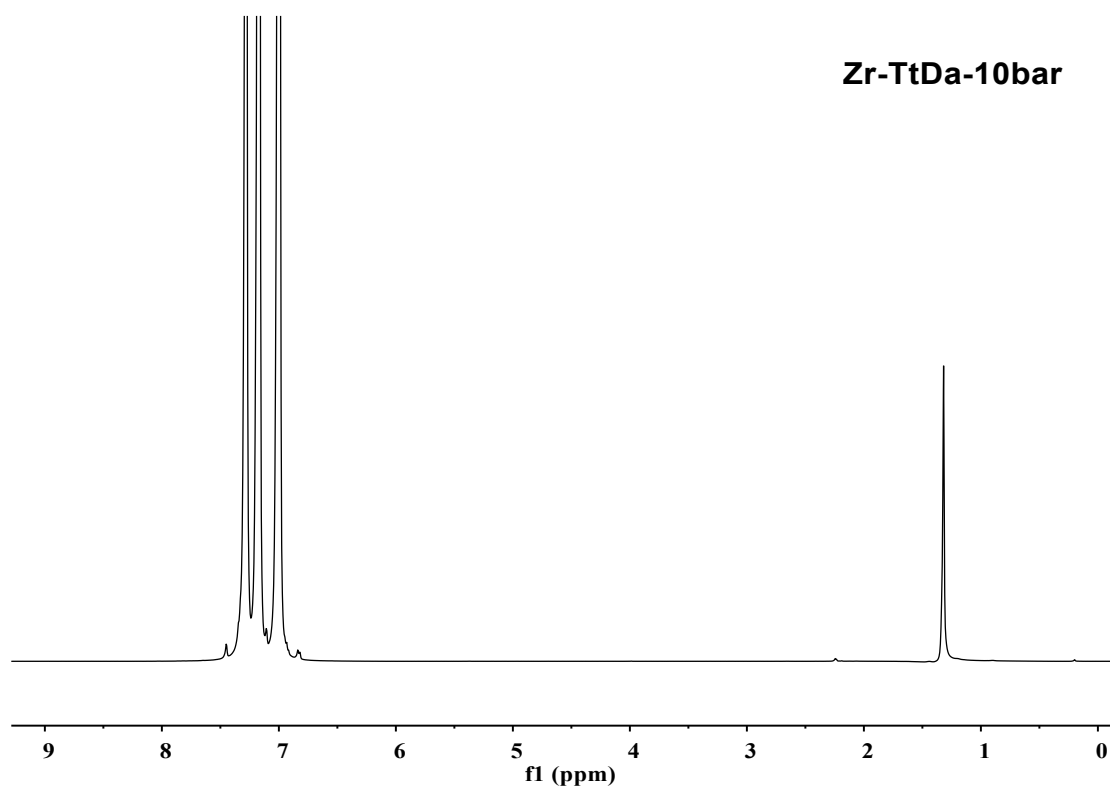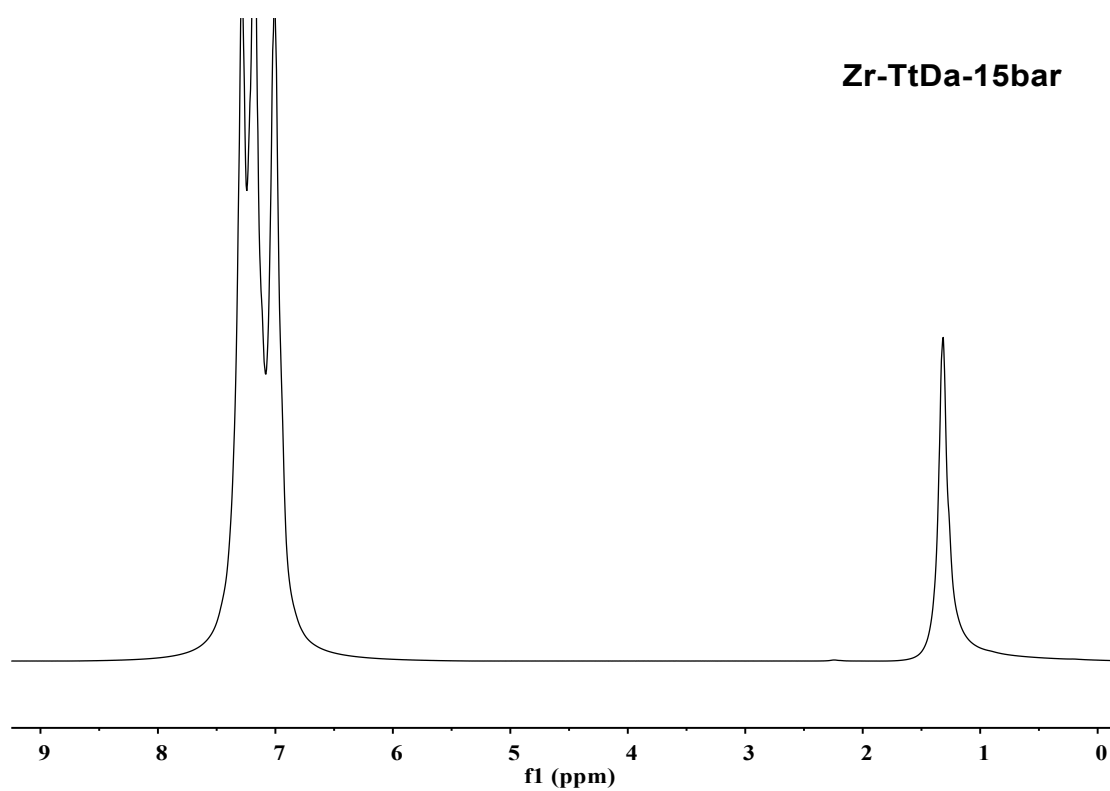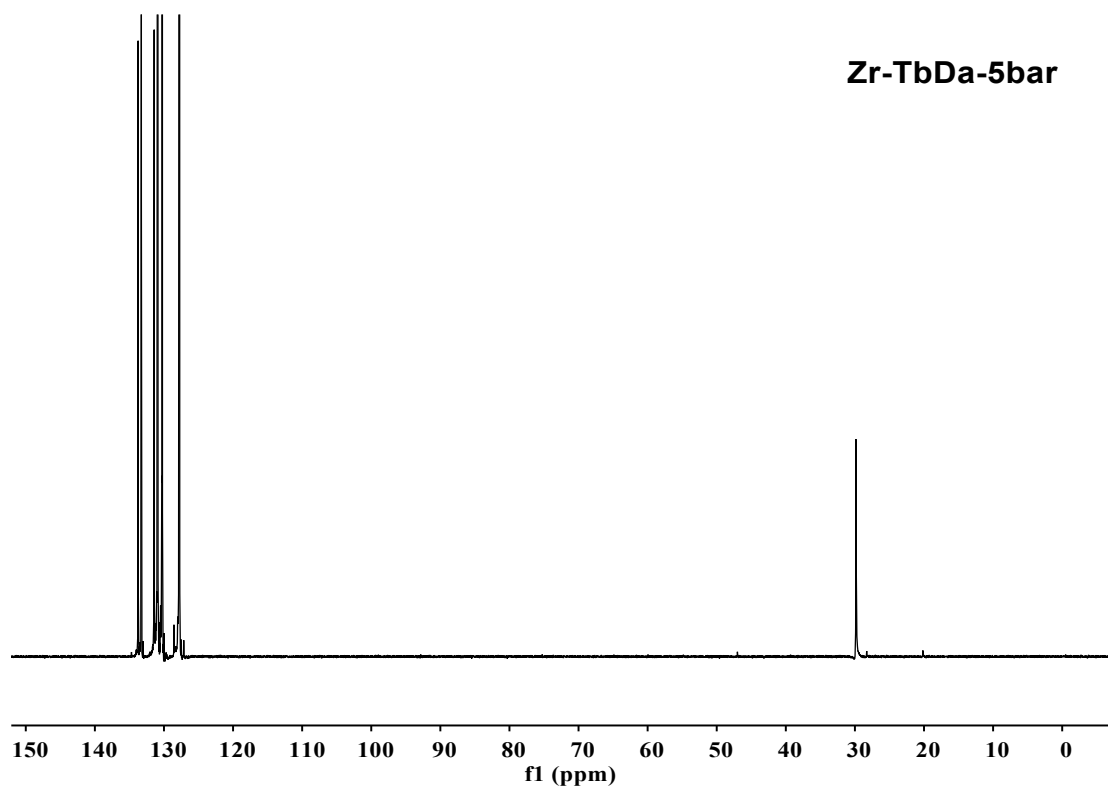
Zr-TbDa-10bar

Figure S28. ^{1}H NMR spectrum of polyethylene produced from Zr-TbDa (500 MHz, 1,2,4-Trichlorobenzene, 125°C). Table 1, entry 2.

Figure S29. ^{1}H NMR spectrum of polyethylene produced from Zr-TbDa (500 MHz, 1,2,4-Trichlorobenzene, 125°C). Table 1, entry 3.
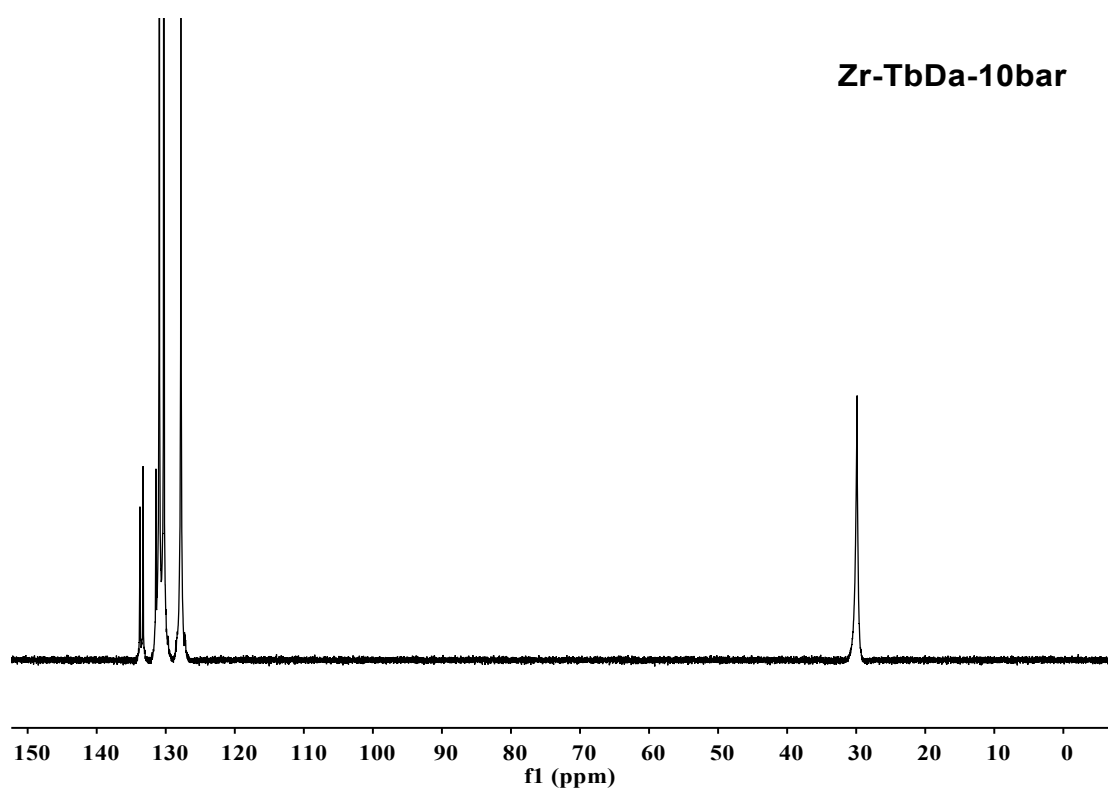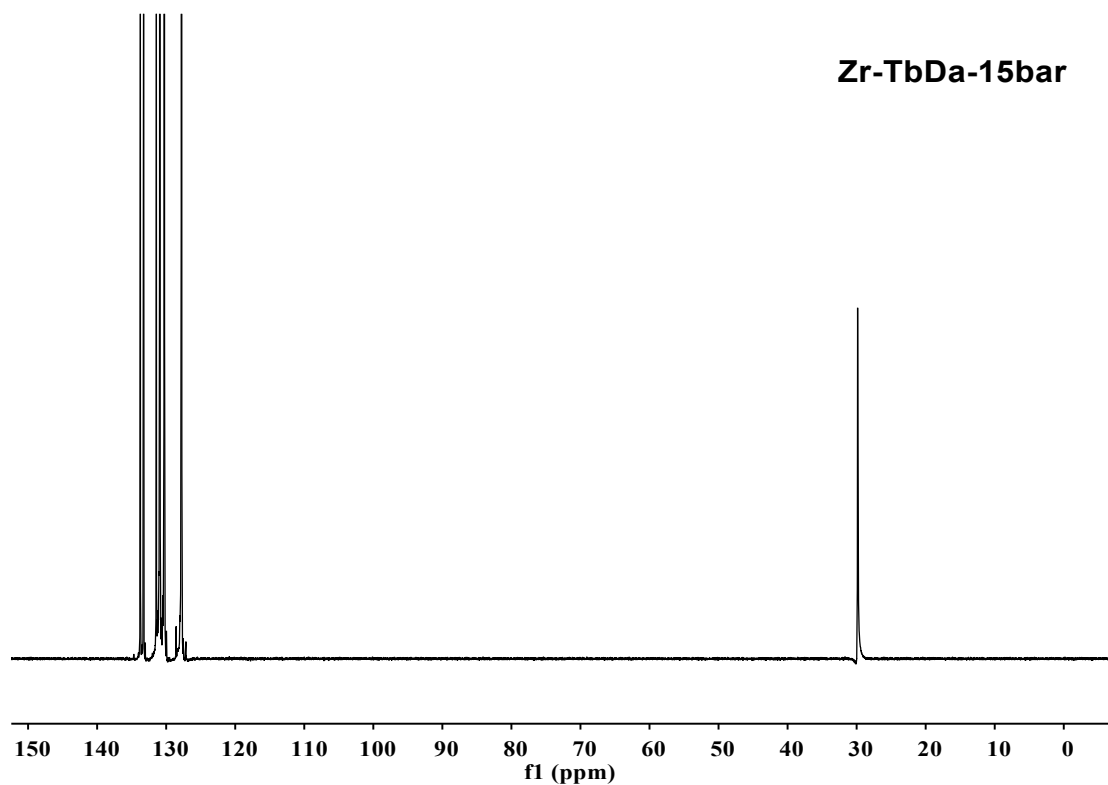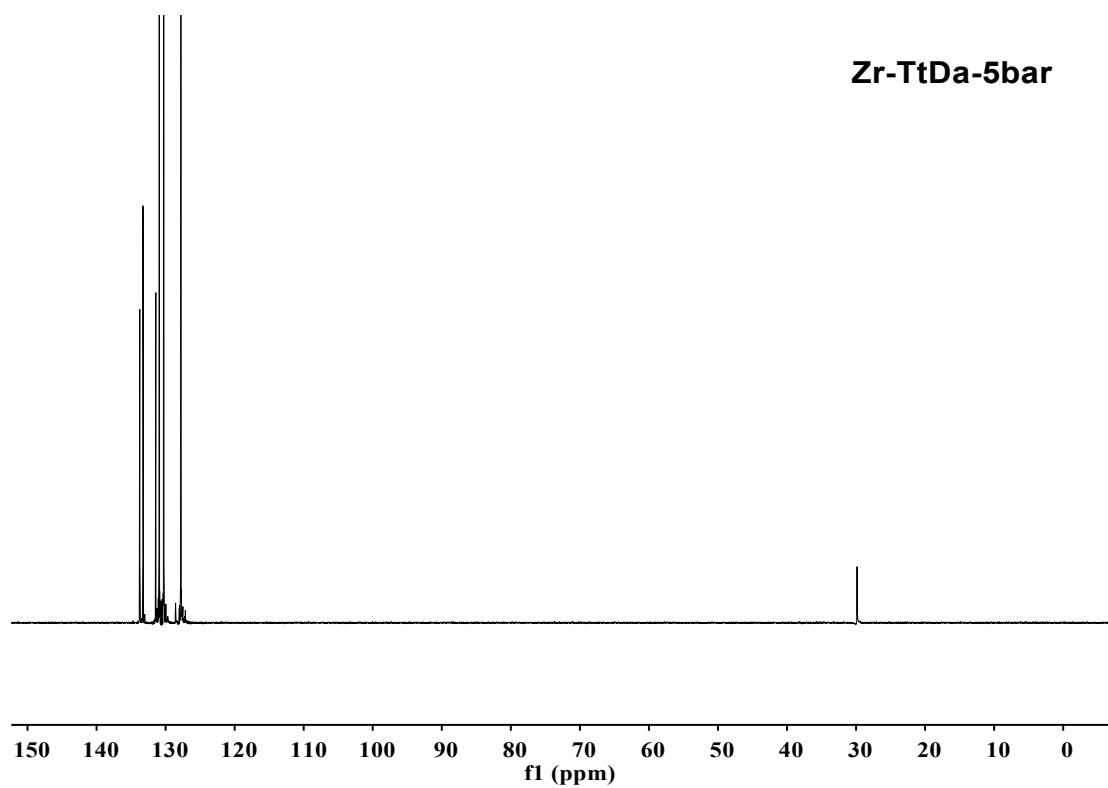

Figure S30. ^{1}H NMR spectrum of polyethylene produced from Zr-TtDa (500 MHz, 1,2,4-Trichlorobenzene, 125°C). Table 1, entry 4.

Zr-TtDa-10bar

Figure S31. ^{1}H NMR spectrum of polyethylene produced from Zr-TtDa (500 MHz, 1,2,4-Trichlorobenzene, 125°C). Table 1, entry 5.

Zr-TtDa-15bar

Figure S32. ^{1}H NMR spectrum of polyethylene produced from Zr-TtDa (500 MHz, 1,2,4-Trichlorobenzene, 125°C). Table 1, entry 6.

Figure S33. ^{13}C NMR spectrum of polyethylene produced from Zr-TbDa (125 MHz, 1,2,4-Trichlorobenzene, 125°C). Table 1, entry 1.
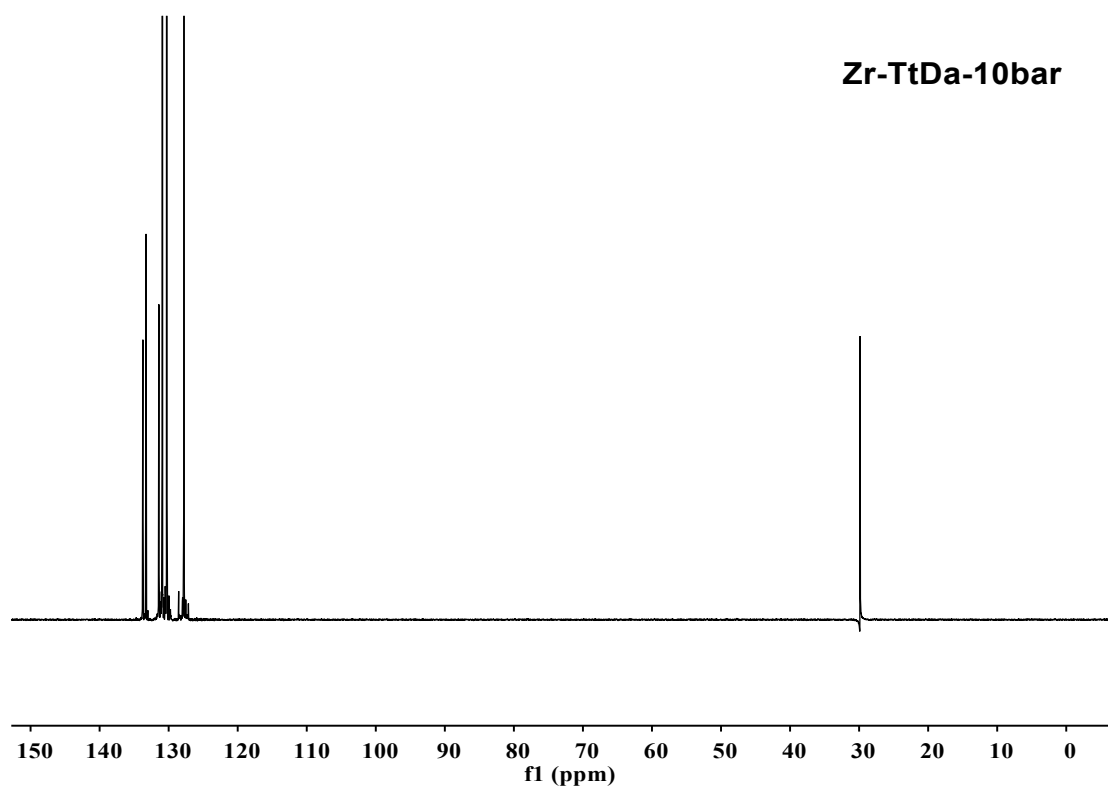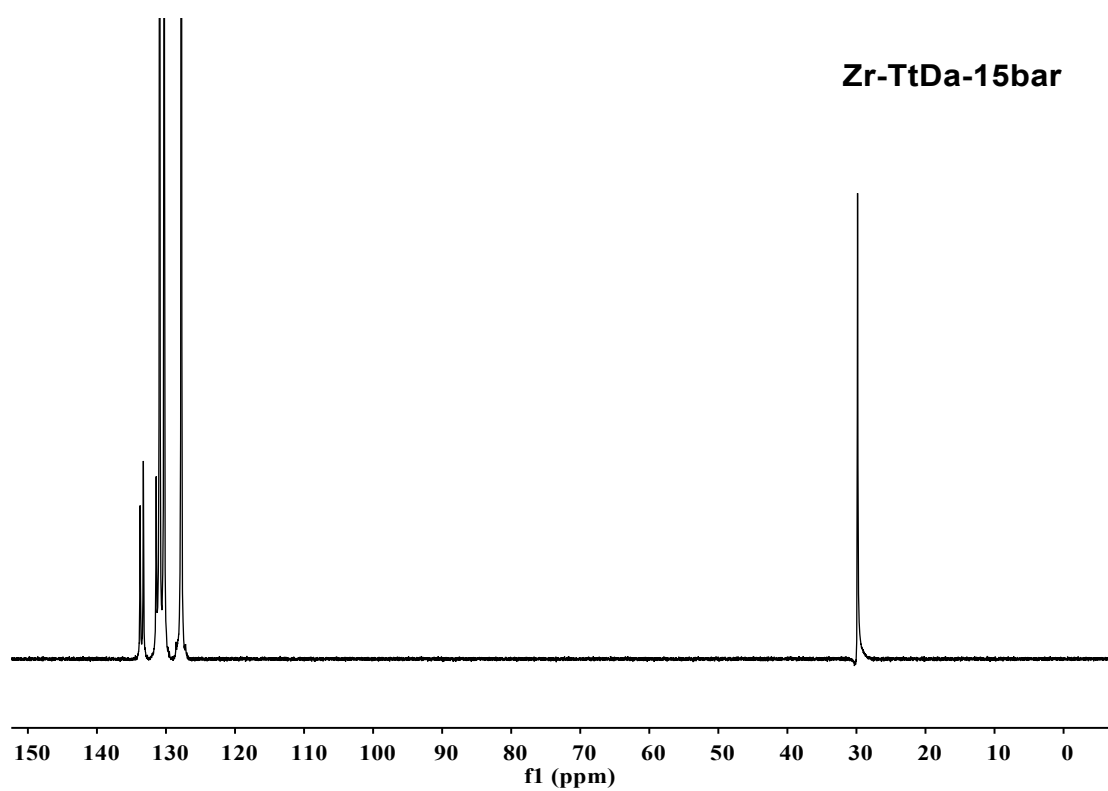

Figure S34. ^{13}C NMR spectrum of polyethylene produced from Zr-TbDa (125 MHz, 1,2,4-Trichlorobenzene, 125°C). Table 1, entry 2.

Figure S35. ^{13}C NMR spectrum of polyethylene produced from Zr-TbDa (125 MHz, 1,2,4-Trichlorobenzene, 125°C). Table 1, entry 3.
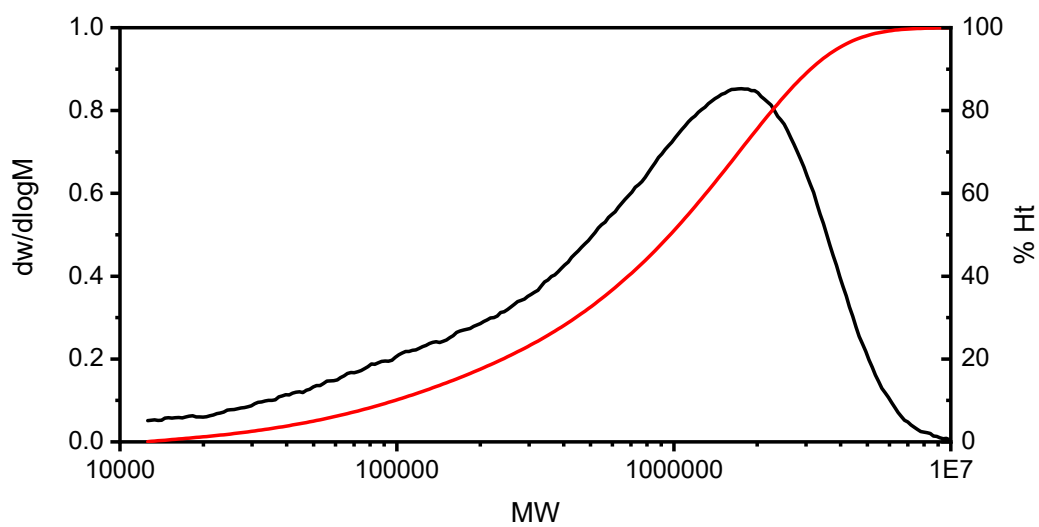

Figure S36. ^{13}C NMR spectrum of polyethylene produced from Zr-TbDa (125 MHz, 1,2,4-Trichlorobenzene, 125°C). Table 1, entry 4.

Figure S37. ^{13}C NMR spectrum of polyethylene produced from Zr-TbDa (125 MHz, 1,2,4-Trichlorobenzene, 125°C). Table 1, entry 5.

Figure S38. ^{13}C NMR spectrum of polyethylene produced from Zr-TbDa (125 MHz, 1,2,4-Trichlorobenzene, 125°C). Table 1, entry 6.

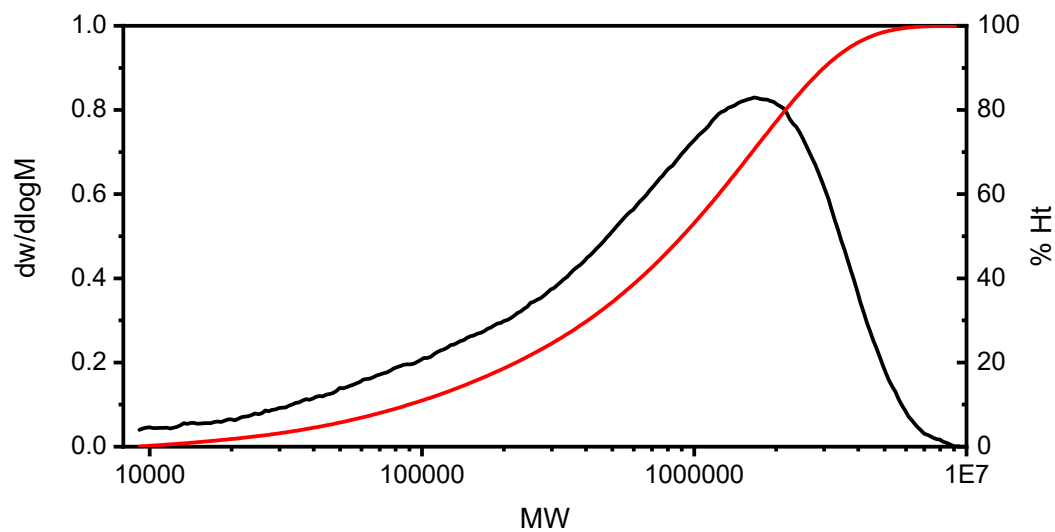**Figure S39.** GPC trace of the polymer from table 1, entry 1.

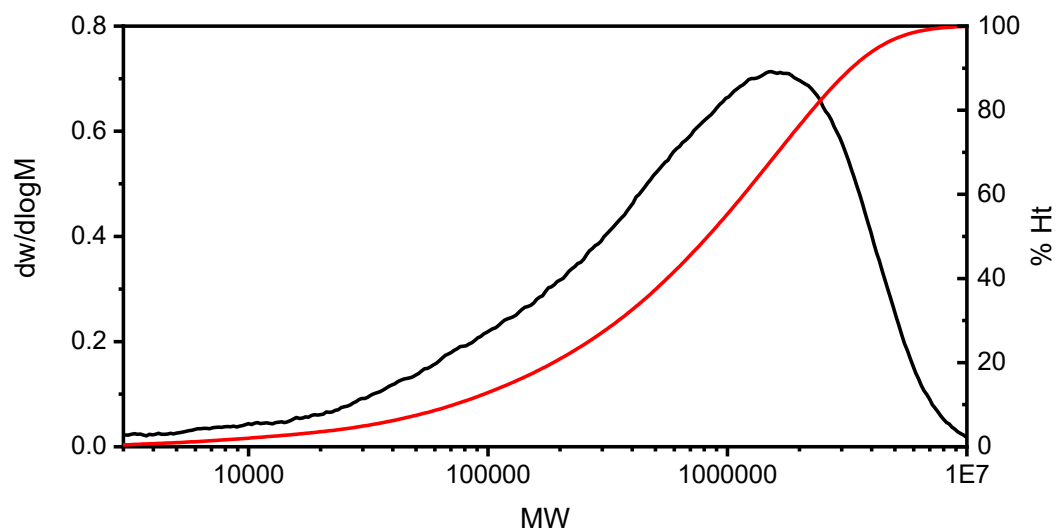**Figure S40.** GPC trace of the polymer from table 1, entry 2.

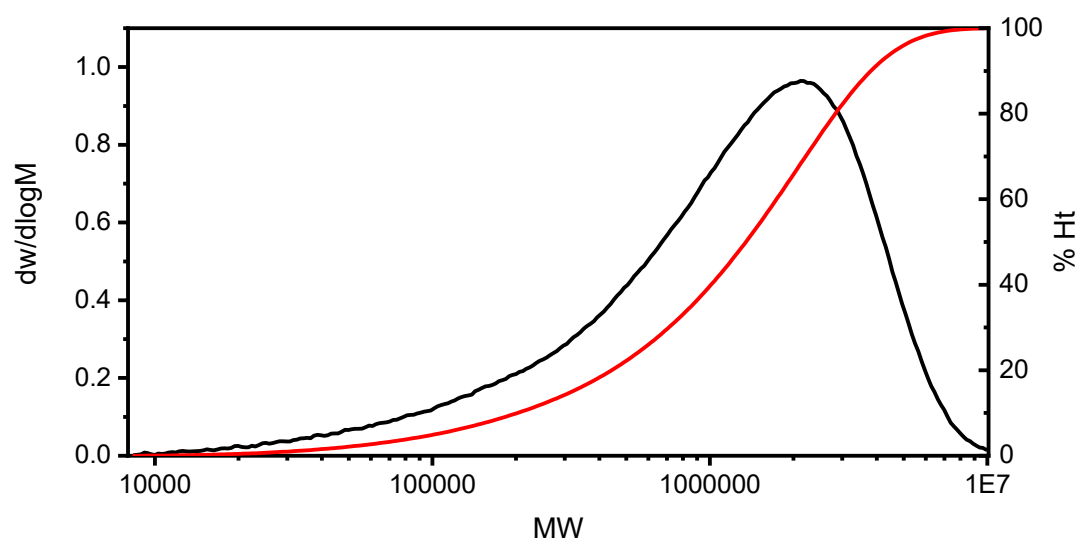**Figure S41.** GPC trace of the polymer from table 1, entry 3.

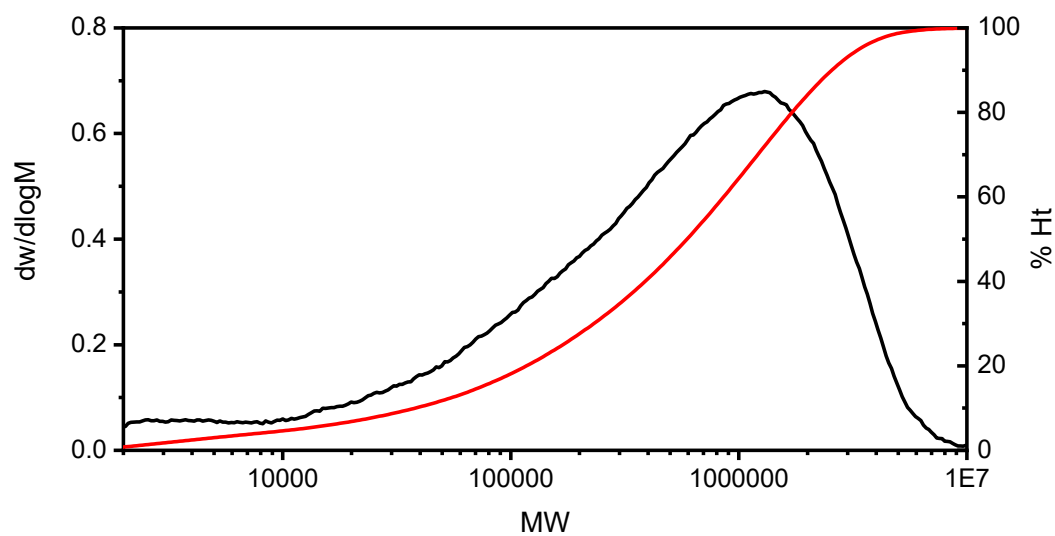**Figure S42.** GPC trace of the polymer from table 1, entry 4.

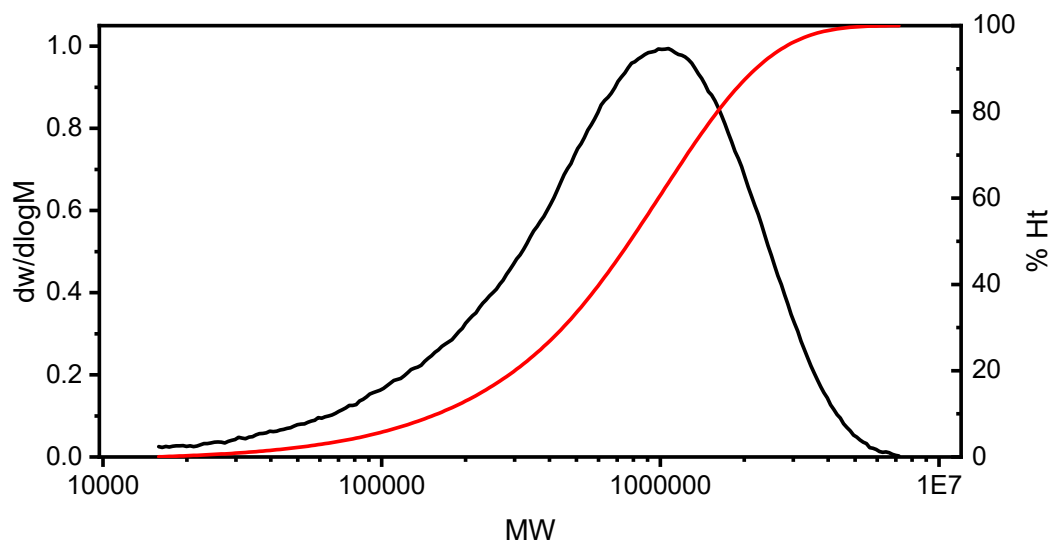**Figure S43.** GPC trace of the polymer from table 1, entry 5.

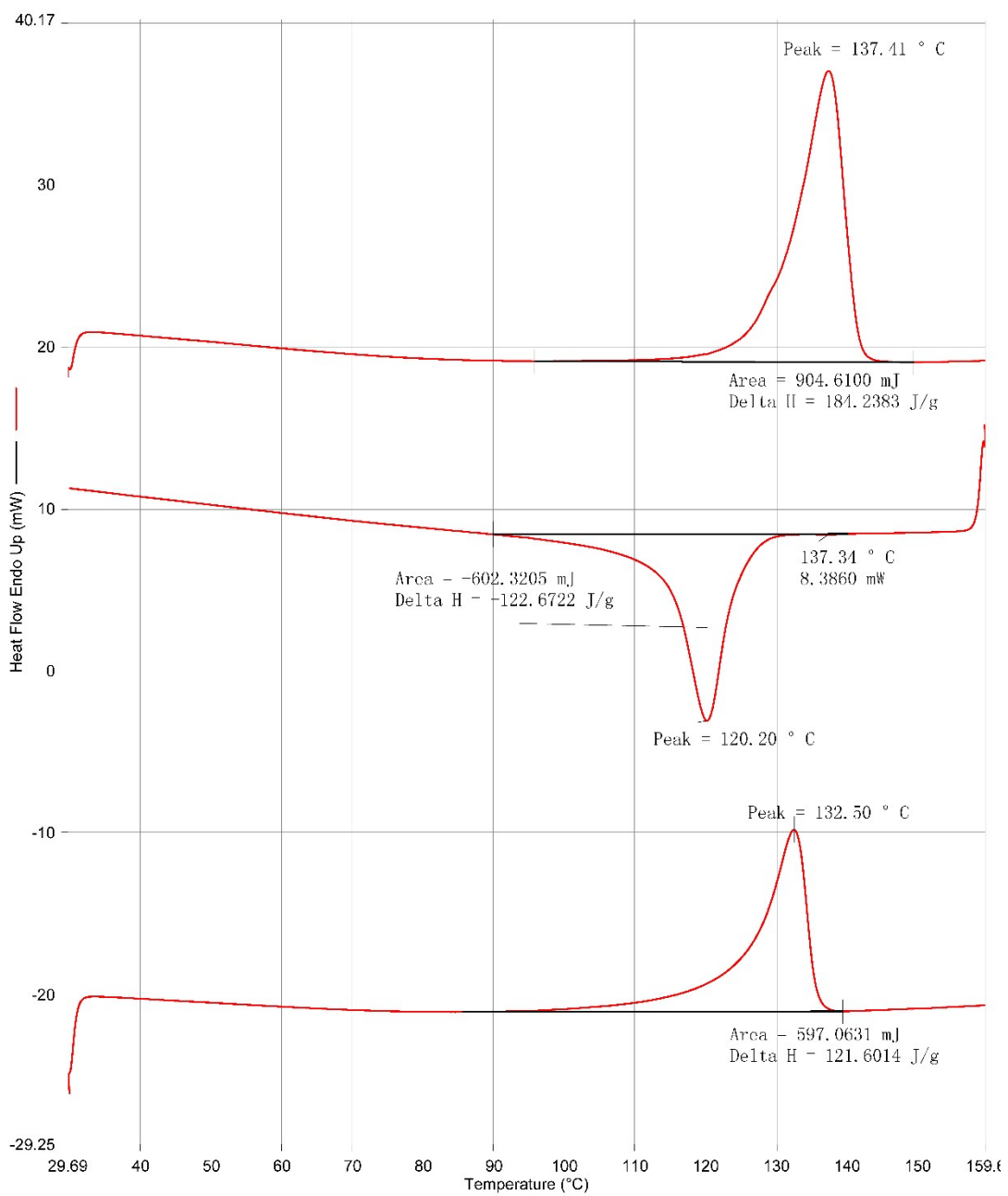**Figure S44.** GPC trace of the polymer from table 1, entry 6.

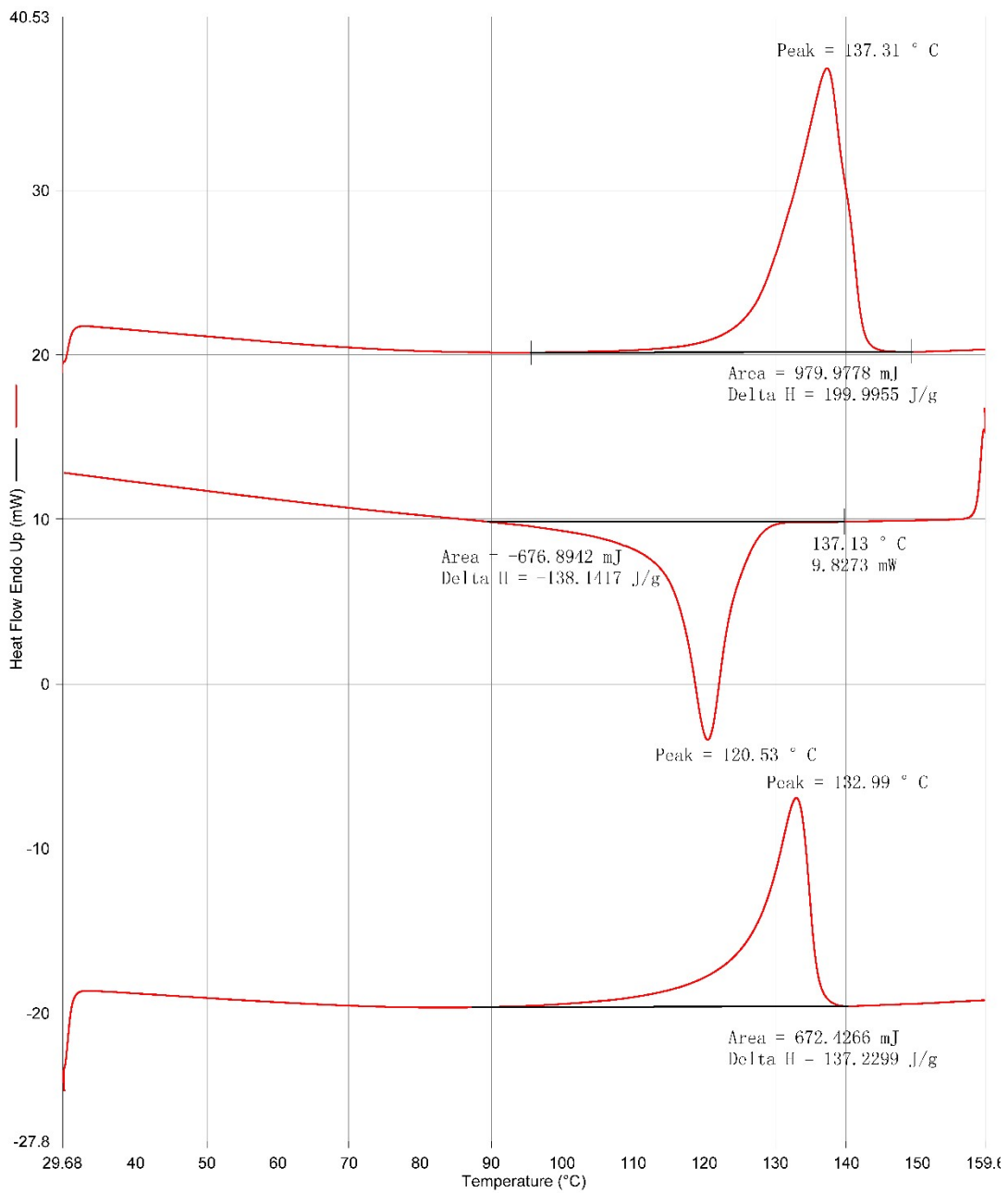**Figure S45.** DSC data of the polymer from table 1, entry 1.

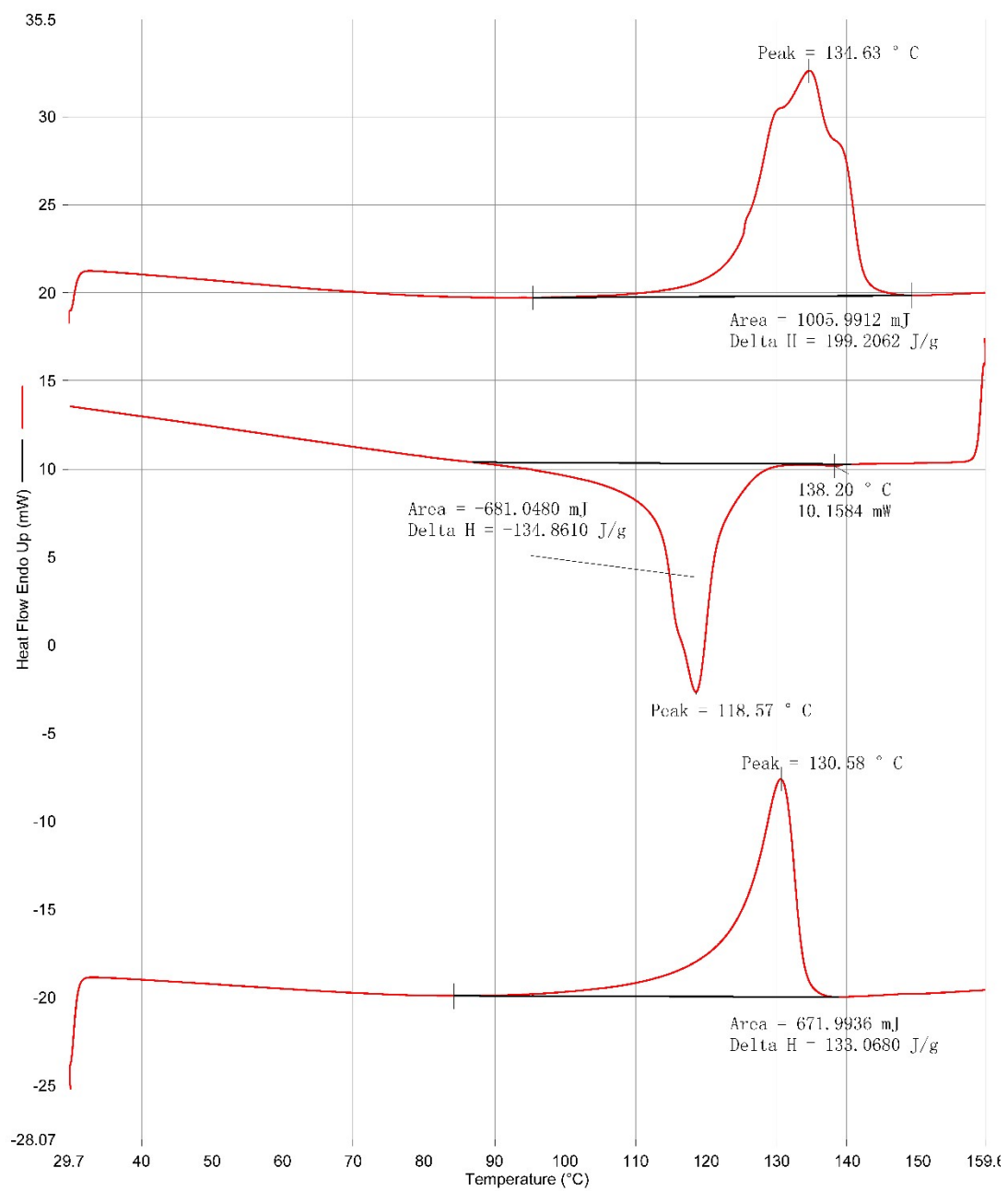**Figure S46.** DSC data of the polymer from table 1, entry 2.

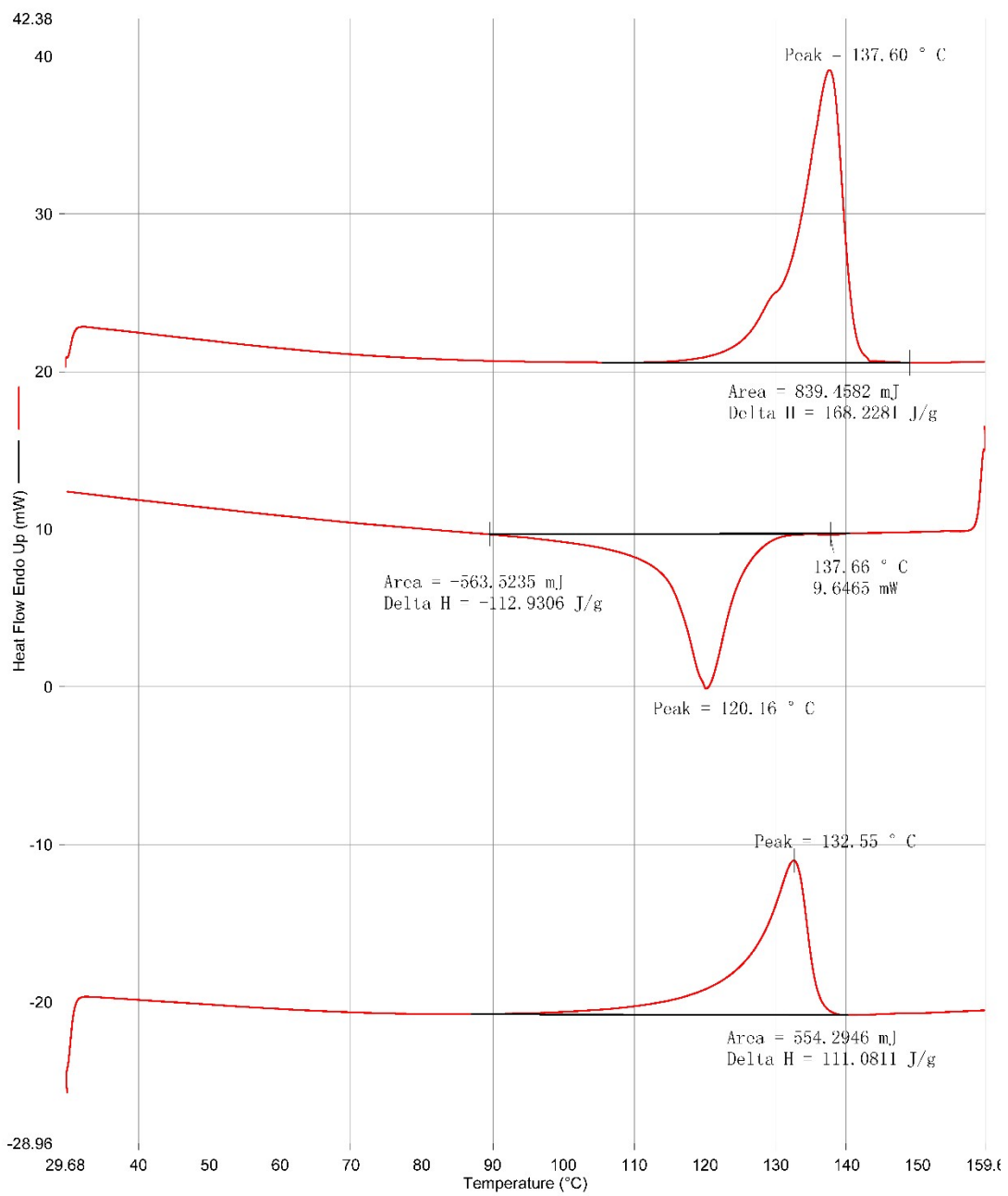**Figure S47.** DSC data of the polymer from table 1, entry 3.

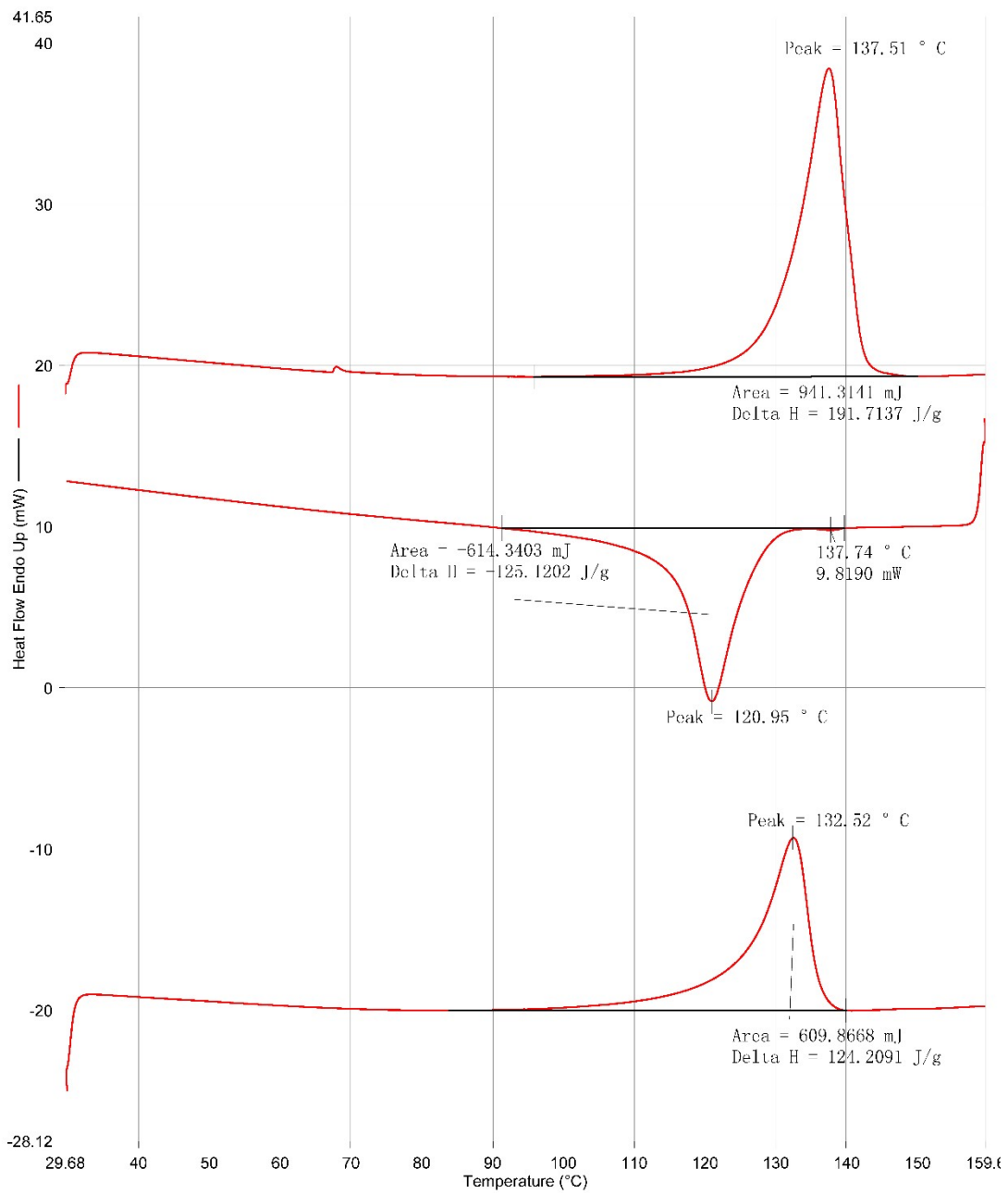**Figure S48.** DSC data of the polymer from table 1, entry 4.

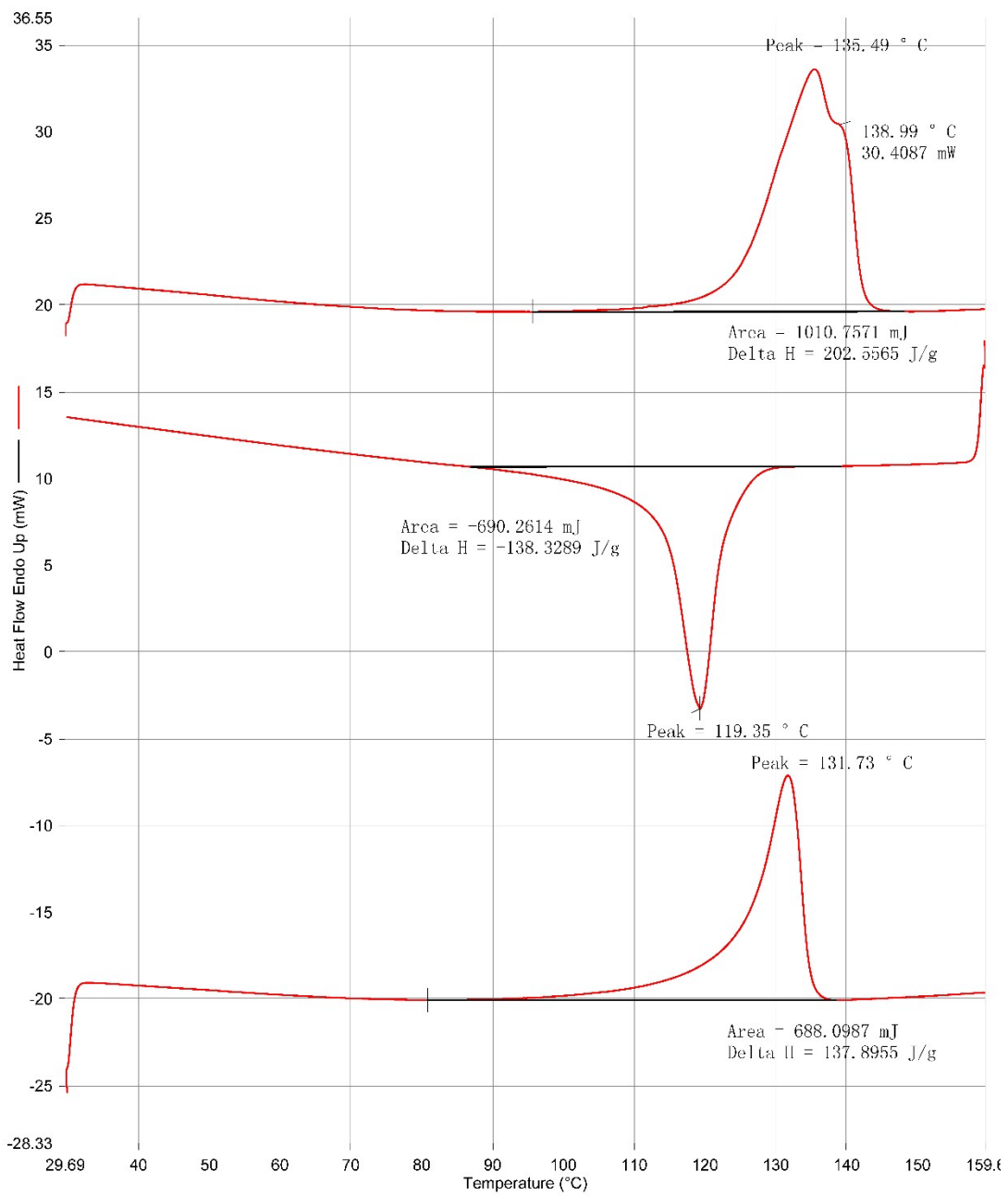**Figure S49.** DSC data of the polymer from table 1, entry 5.

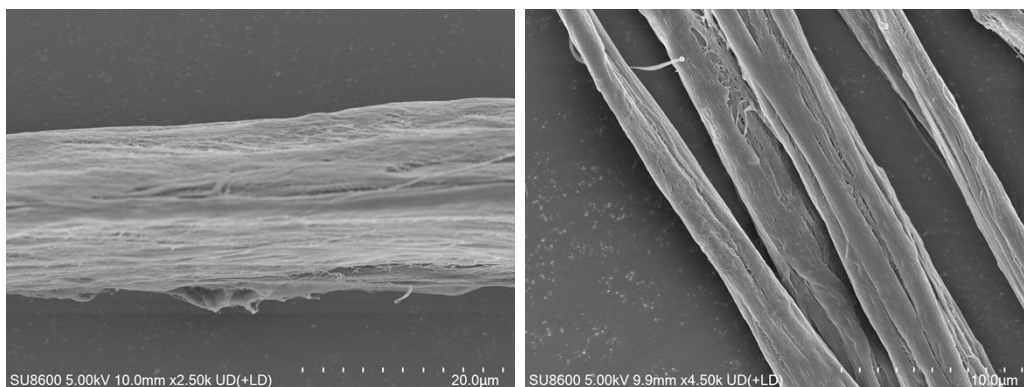**Figure S50.** DSC data of the polymer from table 1, entry 6.

Figure S51. SEM analysis of polyethylene produced by **Zr-TbDa** at 5 bar.
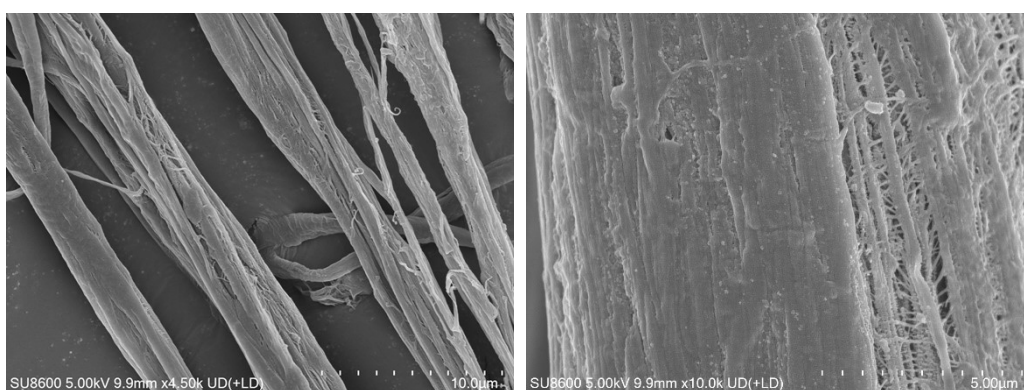
(Table 1, entry1)

Figure S52. SEM analysis of polyethylene produced by **Zr-TtDa** at 5 bar.

(Table 1, entry4)

5. Molecular Dynamics Simulation and DFT calculation

In Material studio (MS), the simulation system was constructed with Universal force field and according to the experimental conditions (100°C, 10 bar ethylene pressure), the relaxation was carried out sequentially in NVE, NPT and NVT tethers with a step size of 0.5 fs, and 30,000 steps under each tether with a relaxation time of 15 ps, and finally the ethylene around the benzene-ring node and triazine node was statistically calculated in order to obtain the radial distribution.
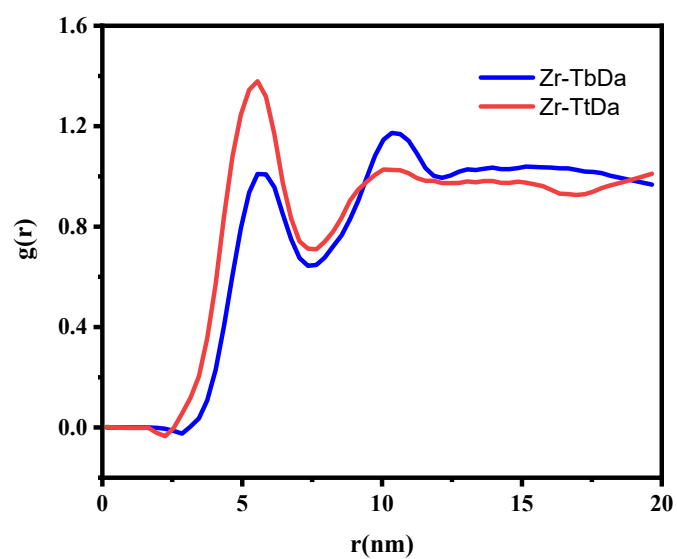
Figure **S53**. Radial distribution of ethylene concentration around benzene ring nodes and triazine linkages of Zr-TtDa and Zr-TbDa fragments.
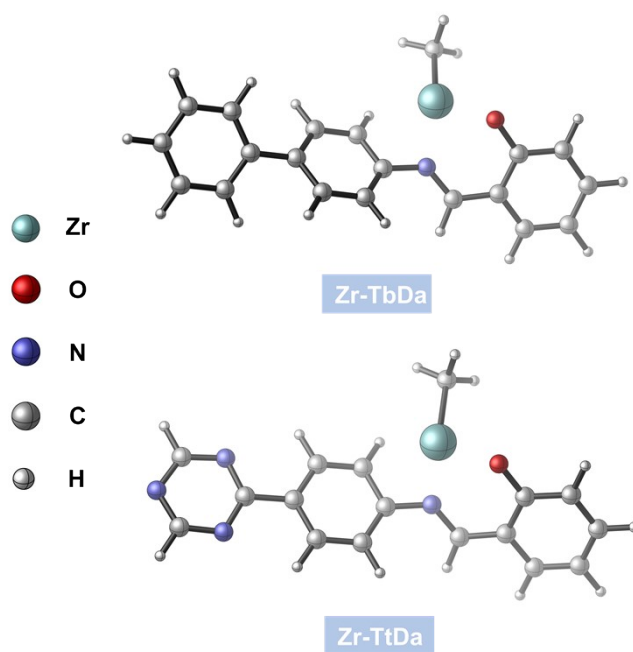

Figure S54. Simplified homogenous models applied for DFT calculations.

6. Reference

(1) Li, Z.; Sun, L.; Zhai, L.; Oh, K. S.; Seo, J. M.; Li, C.; Han, D.; Baek, J. B.; Lee, S. Y. Olefin-Linked Covalent Organic Frameworks with Electronegative Channels as Cationic Highways for Sustainable Lithium Metal Battery Anodes. *Angew. Chem., Int. Ed. Engl.* **2023**, *62*, e202307459.

(2) You, Z.; Wang, B.; Zhao, Z.; Zhang, Q.; Song, W.; Zhang, C.; Long, X.; Xia, Y. Metal-Free Carbon-Based Covalent Organic Frameworks with Heteroatom-Free Units Boost Efficient Oxygen Reduction. *Adv. Mater.* **2023**, *35*, e2209129.

(3) Chi, B.; Zhang, L.; Yang, X.; Zeng, Y.; Deng, Y.; Liu, M.; Huo, J.; Li, C.; Zhang, X.; Shi, X.; et al. Promoting ZIF-8-Derived Fe–N–C Oxygen Reduction Catalysts via Zr Doping in Proton Exchange Membrane Fuel Cells: Durability and Activity Enhancements. *ACS Catal.* **2023**, *13*, 4221-4230.

(4) Barrera, E. G.; dos Santos, J. H. Z. Designing Polyethylene Characteristics by Modification of the Support for FI Catalyst. *Molecular Catalysis* **2017***, 434*, 1-6.

(5) Zhu, B.; Liu, K.; Luo, L.; Zhang, Z.; Xiao, Y.; Sun, M.; Jie, S.; Wang, W. J.; Hu, J.; Shi, S.; et al. Covalent Organic Framework-Supported Metallocene for Ethylene Polymerization. *Chemistry* **2023**, *29*, e202300913.

(6) Yu, F.; Yang, Y.; He, D.; Gong, D.; Chen, Z.-R. Pressure-Sensitive Supported FI Catalyst for the Precise Synthesis of Uni- and Bimodal Polyethylene. *Ind. Eng. Chem. Res.* **2017**, *56,* 4684-4689.

(7) Parveen, R.; Cundari, T. R.; Younker, J. M.; Rodriguez, G.; McCullough, L. DFT and QSAR Studies of Ethylene Polymerization by Zirconocene Catalysts. *ACS Catal.* **2019**, *9*, 9339-9349.